

THE HAGUE UNIVERSITY OF APPLIED SCIENCES

FACULTY: GEZONDHEID, VOEDING EN SPORT

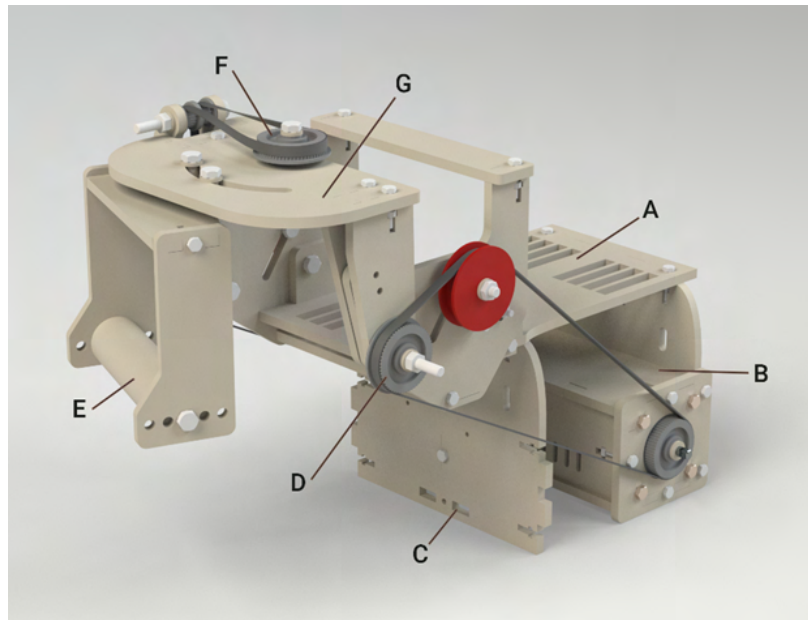
---

# Reliability research of a motion guidance device for the wrist

A RELIABILITY STUDY OF THE MOVEMENTS OF A MOTION GUIDANCE DEVICE FOR THE STANDARDIZATION OF MEASURING WRIST KINEMATICS IN A 4D CT SCAN

---

BACHELOR THESIS - HEALTH TECHNOLOGIES



*Author:*  
Gwen HOGENBOOM

*Supervisors:*  
A. LAGERBERG  
N. MATHIJSEN  
G. KRAAN

*Second evaluator:*  
H. FABER

June 14, 2023

# Reliability research of a motion guidance device for the wrist

A reliability study of the movements of a motion guidance device for the standardization of measuring wrist kinematics in a 4D CT scan

by

Gwen Hogenboom

## Abstract

**Introduction:** There is currently no standardized method for measuring wrist kinematics in a 4D CT scanner. Various methods of wrist motion during a 4D CT scan have been reported in the literature, including asking the patient to move the wrist or using a motion guidance device. No research was done into the reliability of these motion guidance devices. **Purpose:** The purpose of this study was to investigate the reliability of motion guidance during flexion-extension and radial-ulnar deviation to eventually implement the device in the research setting. **Methodology:** Measurements of the movements generated by the device were taken in two conditions; unloaded (without anatomical specimen) and loaded (with anatomical specimen) with the *OptiTrack* equipment. These conditions were tested during flexion-extension and radial-ulnar deviation, with cluster makers placed on the rotation axes of the device. **Results:** During both flexion-extension and radial-ulnar deviation, unwanted movements occurred. Furthermore, a low degree of reliability was found between the two conditions during both flexion-extension and radial-ulnar deviation. **Discussion:** Future research should focus on increasing the reliability of the device by making adjustments to optimize the device. In addition, the effect of the unreliability of the movements generated by the device on the angles between the carpal bones on CT images should be investigated. **Conclusion:** The motion guidance device does not provide reliable data between the two conditions. Without adjustments to improve the reliability of the motion guidance device, its use in future research on wrist kinematics is not recommended.

# Contents

<b>1</b>	<b>Introduction</b>	<b>1</b>
<b>2</b>	<b>Methodology</b>	<b>3</b>
2.1	Initial testing . . . . .	3
2.2	Specimen . . . . .	5
2.3	Variables: movement and marker placement . . . . .	5
2.3.1	Movements generated by the device . . . . .	5
2.3.2	Marker Placement . . . . .	6
2.4	Experimental setup . . . . .	7
2.4.1	Unloaded experiment . . . . .	7
2.4.2	Loaded experiment . . . . .	8
2.5	Data processing for both experiments . . . . .	9
2.6	Data analysis . . . . .	9
2.6.1	Measurement of unwanted movements . . . . .	10
2.6.2	Difference between the two conditions . . . . .	10
2.6.3	Reliability of the movements generated by the motion guidance device	10
<b>3</b>	<b>Results</b>	<b>10</b>
3.1	<i>OptiTrack</i> measurement . . . . .	11
3.2	Measurement of unwanted movements . . . . .	11
3.2.1	Difference between the two conditions . . . . .	12
3.2.2	Reliability of the movements generated by the motion guidance device	13
<b>4</b>	<b>Discussion</b>	<b>15</b>
<b>5</b>	<b>Conclusion</b>	<b>17</b>
	<b>References</b>	<b>18</b>
	<b>Appendices</b>	<b>20</b>
<b>A</b>	<b>Measurement protocol <i>OptiTrack</i> measurement</b>	<b>20</b>

<b>B Measurement protocol 4D CT</b>	<b>27</b>
<b>C All results</b>	<b>35</b>
<b>D Matlab script</b>	<b>36</b>
<b>E Arduino script</b>	<b>45</b>
<b>F Planning</b>	<b>49</b>

# 1 Introduction

Almost all daily activities require movement of the wrist. An injury to the wrist can have a significant impact on a person's life and limits daily activities. The wrist consists of eight carpal bones, three of which articulate with the distal radius and ulna. The eight carpal bones are divided into a proximal- (scaphoid, lunate, and triquetrum bones) and distal row (trapezium, trapezoid, capitate, and hamate bones). This makes the wrist one of the most complex joints in the body. The complexity of the wrist is also due to the kinematic relationships between the carpal bones, tendon structures, ligaments- and neurovascular structures. The complexity of the wrist makes it difficult to diagnose the specific condition and results in difficulties in formulating the correct treatment plan. Incorrect diagnosis and/or treatment can result in permanent damage to the wrist (Kawamura & Chung, 2007).

A detailed understanding of the normal and abnormal kinematics of the wrist is essential for the correct diagnosis of wrist injuries and the development of a treatment plan. Physical examination and radiography are used to diagnose wrist injuries. Kinematics were previously measured by static ulnar-radial deviation and flexion-extension of the wrist during a radiograph. The limitation of this technique is the inability to measure all six degrees of freedom of the rotations and translations that occur between the carpal bones. Other more modern techniques for measuring and visualizing wrist kinematics are computed tomography (CT) and magnetic resonance imaging (MRI). Similar to radiography, these newer techniques are not able to measure the full range of wrist kinematics, because the technique is limited by the acquisition of wrist positions during a series of static positions along a path of motion (Andersson et al., 2015; Kamal et al., 2016; Moojen et al., 2003; Prosser et al., 2011). This suggests that there is no 'golden standard' for measuring and visualizing wrist kinematics.

In a previous review, Crezee (2022) describes and compares seven techniques for measuring wrist kinematics under dynamic conditions. Crezee (2022) considers the following factors: accuracy, harm to patient/anatomical specimen and sample frequency. Four-dimensional computed tomography (4D CT) is cited as the most capable method for measuring carpal kinematics. Kamal et al. (2016) and Kwong et al. (2015) support this conclusion. 4D CT scans generate 3D images over time (Brinkhorst et al., 2021). In addition, Brinkhorst et al. (2022) demonstrated that this method is particularly reliable for measuring carpal kinematics in vivo in an unaffected wrist. At present, 4D CT scanning is an experimental tool and is not yet used in a clinical setting.

There is currently no standardized method for measuring wrist kinematics in a 4D CT scanner. Various methods of moving the wrist during a 4D CT scan have been reported in the literature, asking patients to move the wrist (Rauch et al., 2018) or using a motion guidance device (White et al., 2019) with an anatomical specimen. There is virtually no standardized method of moving the wrist in a CT scanner or a reliable motion guidance

device, therefore previous research is difficult to compare (Brinkhorst et al., 2022; White et al., 2019).

In order to contribute to the literature Crezee (2022) described the development process of a motion guidance device. The device is displayed in figure 1. The motion guidance device performs motorized flexion-extension and radial-ulnar deviation movements.

The motion guidance device is developed to measure wrist kinematics and can provide a standardized method to measure the kinematics. In another study within the Reinier Haga Orthopedic Centre (RHOC) a new 3D printed implant for the lunate bone is being developed. To test, the implant is

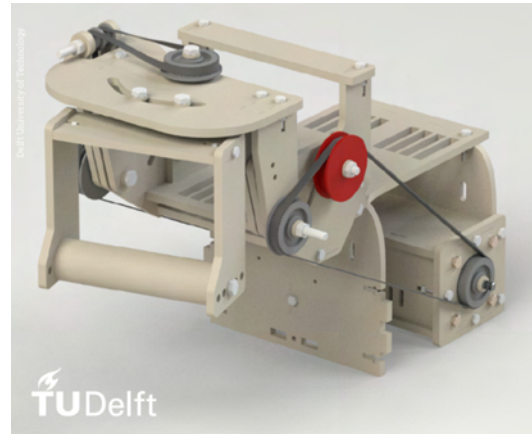


Figure 1: The motion guidance device (Crezee, 2022)

placed in an anatomical specimen, before it is tested on live subjects. In order to test the behavior of this new implant relative to the other carpal bones, 4D CT scans have to be made. The specimen has to be moved automatically, the motion guidance device can be used for this purpose. The usage of the device to generate automatic movements during a 4D CT-scan of flexion-extension and radial-ulnar deviation connects the separate study's. The end goal of Crezee (2022) research is to help evaluate the wrist kinematics of the newly developed lunate bone during a 4D CT-scan. Before the device can be used for measuring the kinematics of the developed lunate bone, the movements generated by the device should provide reliable data.

This research focuses on the reliability of the motorized movements (flexion-extension and radial-ulnar deviation) generated by the motion guidance device as well as the impact of the weight of an anatomical specimen (the loaded condition). This is the first step that could lead to the implementation of the device in the research setting. The second step can start when the movements generated by the device provide reliable data.

The second step includes comparing 4D CT-scans of anatomical specimen to examine whether the movement of the device is fully transferred to the wrist, the description and execution of the second step falls outside the scope of this research. The second step can start when the movements generated by the device are proven to provide reliable data, which is step one.

The way in which the reliability of the motorized movements (step one) will be tested is as follows: first, the reliability of the device is tested by performing the flexion-extension and radial-ulnar deviation under unloaded (without anatomical specimen) and loaded conditions (with anatomical specimen). Second, the movements generated by the device are tested to ensure that the device rotates under the same angles with repeated movements

and does not show unwanted movements around other axes. Third, it is tested to what extent the movement angles generated around the flexion-extension and radial-ulnar deviation axes match in the loaded and unloaded conditions.

So, the main objective of this research is to test the reliability of the movements generated by the device and the data that it provides. The research question supporting the above is as follows: *Do the flexion-extension and radial-ulnar deviation, which are motor driven movements generated by the motion guidance device, provide reliable data in two conditions; unloaded and loaded?*

This research will be the start of research into the reliability of the movements generated by the motion guidance device. The movements of the device are expected to be reliable in the unloaded condition. Thereby, it is expected that the anatomical specimen will create resistance that may cause the desired angular excursions to no longer be achieved.

## **2 Methodology**

This section describes the methodology for testing the reliability of the movement generated by the motion guidance device. The described experiments are designed to collect quantitative data about the movements generated by the device in an unloaded- and loaded condition. Information is provided on the initial testing, the movements of the device and marker placement, the anatomical specimen, experimental setup (unloaded and loaded), data collection and the data analysis.

### **2.1 Initial testing**

The device was tested before the experiment took place to ensure it worked as described in the previous documentation. After testing the device in the unloaded condition, it did not work sufficiently. Before going over the insufficiencies, an overview of all the components is given in figure 2.

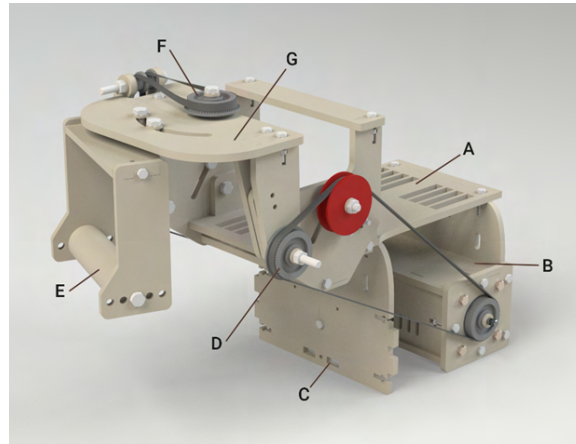


Figure 2: Overview of the motion guidance device

*“A) Plateau for the arm to rest on, with slots for Velcro straps to pass through. B) Stepper motor housing with two bipolar NEMA 23 stepper motors. C) Holes for attaching the unit to a wooden board. D) Toothed belt assembly for flexion/extension. E) Swivel arm with bar for holding or attaching the hand. This part swivels left and right. F) Toothed belt assembly for ulnar and radial deviation. G) Main carriage. This part will move forward and backward.” (Crezee, 2022).*

Several problems surfaced after initial testing:

1. The timing belts were too loose (figure 2D).
2. The screws connected to the pulleys bend.
3. Two timing belts, on the side of radial-ulnar deviation movement, move over both gears (figure 2F).

Adjustments were made to the device and Arduino script (controlling the motors) after initial testing in order for the device to work. The updated Arduino script can be found in appendix E. The solutions to the problems were:

1. Increasing the inside diameter of the pulleys to tighten the timing belts (figure 3B).
2. Developing a suspension to prevent the screw from bending (figure 3A).
3. Making a higher edge between the two gears on the side of radial-ulnar deviation (figure 4).

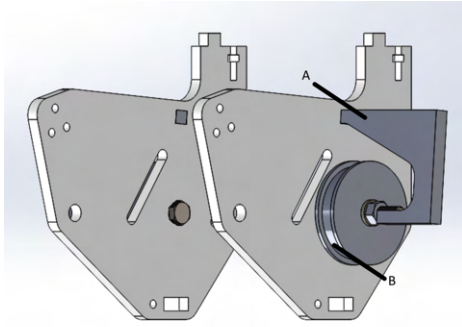


Figure 3: Adjustments device



Figure 4: Adjustment radial-ulnar deviation gear, part of figure 2F

## 2.2 Specimen

The RHOC Medical Ethics Committee gave local approval for the use of five anatomical specimens for measurement with the *OptiTrack* system. This number of anatomical specimens was chosen according to the availability. More than one anatomical specimen must be tested (Mat Jais et al., 2014). The anatomical specimens were amputated above the elbow and below the shoulder. The anatomical specimens had no known history of wrist injury or other pathology, of which only one specimen was left-handed. The device is made so left, and right-handed specimen can make the same movements. The hand is placed in the device with the palm around the bar of the swivel arm (figure 2E).

## 2.3 Variables: movement and marker placement

In this section, the variables used in the experiment are explained. The variables contain the movements generated by the device and the marker placement to track the movements.

### 2.3.1 Movements generated by the device

The device performs motorized flexion-extension and radial-ulnar deviation. Crezee (2022) mentioned the range of motion of the device:  $80^\circ$  extension to  $80^\circ$  flexion;  $-34^\circ$  radial deviation to  $34^\circ$  ulnar deviation. In Crezee (2022) research, the extension only reached  $34^\circ$ .

The movements corresponding with the axes ( $x$ ,  $y$ ) were defined with the help of Jensen et al. (2021); de Roo et al. (2020). In the loaded condition (with the anatomical specimen in position), the axes were aligned with the wrist axes of the specimen. This is verified by performing test measurements of both movements. The axes are displayed in figure 5. The maximum (+) and minimum (-) angles of the rotations are given in table 1. The rotations around the  $z$ -axis were also included in the analysis to see if any movement occurs around

this axis.



X = Flexion-Extension; Y = Radial-Ulnar Deviation

Figure 5: Movements corresponding with axes of the device

Table 1: Movements corresponding with axes of the device (figure 5)

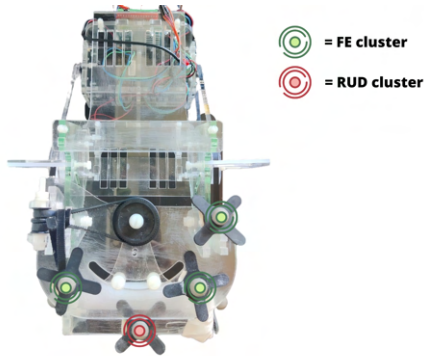
Movement	axis
Extension	(+) x
Flexion	(-) x
Ulnar Deviation	(+) y
Radial Deviation	(-) y

### 2.3.2 Marker Placement

The marker placement is determined by the axes of rotation and the visual obstruction caused by the device. Given the movements of the device and the end objective of this study, cluster markers are the best choice for measuring the movements around all axes. The cluster markers provide 3D data instead of 2D. Although the device rotates around a single axis (only flexion-extension or radial-ulnar deviation) during the movements, 3D registration of the movements is preferred. Rotations in another plane may occur that would go unnoticed with 2D analysis. In addition, in future research, the aim is to track the movements of the hand itself.

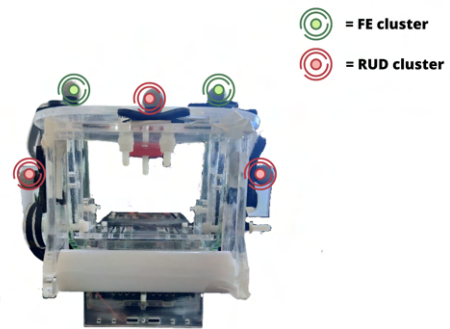
Cluster markers were placed on the device and were assigned in the Motive 2.2.0 software (*OptiTrack*, NaturalPoint, Inc., Oregon, OR, USA). The names: RUD (radial-ulnar devia-

tion) and FE (flexion-extension) were used to name the clusters in the software. When clusters are mentioned further in the study, they are referred to by these names. The cluster markers were positioned on the parts of the device that rotate about the flexion-extension axis or about the radial-ulnar deviation axis, as is seen in figures 6 & 7. For each measurement only the cluster of concern was analyzed, during flexion-extension only the FE cluster and during radial-ulnar deviation, only the RUD cluster. In the RUD cluster movement was expected around (+,-) y-axis and for FE around the (+,-) x-axis, defined in table 1 and figure 5. The non-moving part of the device was firmly secured, therefore no cluster was added to this part of the device.



Green = FE cluster; red = RUD cluster

Figure 6: Aerial view - placement of reflective markers FE cluster



Green = FE cluster; red = RUD cluster

Figure 7: Frontal view - placement of reflective markers RUD cluster

## 2.4 Experimental setup

The experimental setup consists of two separate testing conditions: unloaded (without anatomical specimen) and loaded (with anatomical specimen). When referring to these specific conditions, unloaded and loaded are used to indicate which condition it is about.

### 2.4.1 Unloaded experiment

The measurements of the unloaded experiment were conducted in the movement laboratory in the basement of the Haagse Hogeschool, The Hague.

The experiment starts by placing the device on a table surrounded by the camera setup. The camera setup consists of four *OptiTrack* Flex Cameras mounted on tripods. The four cameras were aimed at the device, as is shown in figure 8. The *OptiTrack* system provides 3-dimensional position data using reflective markers at a sampling frequency of 120 Hz. The *OptiTrack* Flex system was also chosen for its accessibility and portability. The camera setup has to be calibrated before it can track the cluster movements. After the calibration, the cluster markers were placed as described in section 2.3. Flexion-extension and radial-ulnar deviation were both performed 20 times without changes to the environment.



Figure 8: Camera set up - unloaded testing condition

#### 2.4.2 Loaded experiment

In the loaded condition, five anatomical specimens were used to collect the maximum and minimum angles around all axes during both movements. The experiment was conducted in the CT room of the Reinier de Graaf Gasthuis. The experiment starts by securing the device with tie wraps to a wooden board and placing the wooden board on a table surrounded by the camera setup. The camera setup was similar to the setup used for the unloaded experiment, shown in figure 9. The next step was to secure the anatomical specimen to the device with the palm of the hand around the bar of the swivel. The anatomical specimen was further secured by Velcro straps around the arm. The placement of the hand and Velcro straps is shown in figure 10.



Figure 9: Camera setup - loaded condition



Figure 10: Anatomical specimen secured to device

The measurement was performed with an anatomical specimen for both flexion-extension and radial-ulnar deviation. To obtain test-retest reliability, the measurement is repeated three times for both flexion-extension and radial-ulnar deviation, six measurements per specimen. Resulting in thirty measurements in total. The measurement protocol in the loaded condition is shown in the table 2. The whole measurement protocol of the experiment can be found in appendix A.

Table 2: *OptiTrack* measurement protocol.

Measurement	Movement	Plane
1	flexion-extension	sagittal
2	flexion-extension	sagittal
3	flexion-extension	sagittal
4	radial-ulnar deviation	frontal
5	radial-ulnar deviation	frontal
6	radial-ulnar deviation	frontal

## 2.5 Data processing for both experiments

The data analysis was done using SPSS. One of the five specimen was left-handed, the radial-ulnar deviation was reversed in Excel (Version 16, Microsoft, Albuquerque, New Mexico, USA). Missing marker data was reassigned or filled in using the Motive 2.2.0 software. If too much of the position data of the markers was missing, the measurements were removed from the analysis. The raw marker data was exported from the Motive 2.2.0 software to Matlab (Toolbox Release 2019b, The MathWorks, Inc., Natick, Massachusetts, United States). The marker data consists of the  $x$ ,  $y$  and  $z$  position data of three markers per cluster (FE and RUD). The position data was processed using Matlab. The angles of the clusters were calculated using the Cardan-Euler angle method. Euler angles define a rotation in three sequential elementary rotations about orthogonal axes of a Cartesian coordinate system, which use moving axes. The Euler angles were derived using the decomposition order:  $x,y,z$ . Maximum (+) and minimum (-) angles were calculated around each axes per movement. The (+) and (-) angles from each axes per movement were analyzed in SPSS. The Matlab script used to extract the angles is included in appendix D.

## 2.6 Data analysis

The (+) and (-) angles calculated in Matlab were exported from Matlab/Microsoft Excel to IBM SPSS Statistics 27 (IBM SPSS Statistics 27, SPSS, Inc, Chicago, IL, USA). The following three sections discuss three different statistical tests that are in line with categories in the introduction: testing if the movements generated by the device show unwanted movements in other planes during repeated movements; the extent the angles match in a loaded- and unloaded condition; the reliability of the device was tested under an unloaded- and loaded

condition.

### **2.6.1 Measurement of unwanted movements**

For both conditions, the mean and standard deviation (*SD*) of the device's maximum and minimum angles around all axes during flexion-extension and radial-ulnar deviation were calculated. This was done for both conditions to test for movement around unwanted axes. Furthermore, it was tested if the device reaches the maximum limits set by (Crezee, 2022), mentioned in section 2.3.1.

### **2.6.2 Difference between the two conditions**

The difference between the movements generated by the device in the unloaded and loaded condition was calculated using the (+) and (-) angles around all axes. The normal distribution of the maximum and minimum angles around all axes was tested using the Shapiro-Wilk test (subjects < 50). This was done separately for each movement. After testing for normal distribution, angles around all axes for both conditions were compared using the independent t-test if the angle data around all axes were normally distributed ( $p > 0.05$ ). If the angles were not normally distributed, the Mann-Whitney U test was used ( $p < 0.05$ ).

### **2.6.3 Reliability of the movements generated by the motion guidance device**

The test-retest reliability was assessed using Bland-Altman plots and an ICC. The Bland-Altman plots consist of plotting the difference between the measurements in the unloaded and loaded condition against the mean of these measurements, with the 95% limits of agreement ( $\pm 1.96 SD$ ) to the mean difference line (Myles & Cui, 2007). ICC estimates and their 95% confidence intervals were calculated using SPSS statistics based on a single measurement, absolute agreement, 2-way mixed effects model (Koo & Li, 2016). Movements around all axis in both clusters (table 1) were included in the ICC. A value close to 1.0 indicates that the maximum and minimum angles around all axes were consistent and that the test-retest reliability is high, values below 0.5 indicate that the test-retest reliability is low. Negative values can be found, these indicate poor reliability (Giraudeau, 1996).

## **3 Results**

Three different statistical test were conducted, which are in line with the sections in the data analysis: measurement of unwanted movements, the difference between the conditions and the reliability of the movements generated by the device. The findings are step by step explained in the following sections.

Measurements were performed in two conditions: unloaded and loaded. In the loaded

condition, five anatomical specimens were used. The *OptiTrack* data consisted of (+) and (-) angles around three axes in two clusters (FE, RUD). The results are presented in tables 3 to 5 and figures 11 to 20.

### 3.1 *OptiTrack* measurement

To assess the reliability of the movements (flexion-extension and radial-ulnar deviation) generated by the motion guidance device, an experiment was performed in an unloaded and loaded condition. Twenty measurements were taken for both movements in the unloaded condition. Fifteen measurements of flexion-extension were performed with five different anatomical specimens (loaded condition). Fifteen measurements were performed of radial-ulnar deviation, of which twelve were included in the analysis. Three of the fifteen measurements missed a significant part of the marker data, these were excluded from the statistical analysis. There were no unexpected movements detected in the cluster that was fixed to the device. All values were zero or close to zero. This cluster was excluded from the statistical analysis.

### 3.2 Measurement of unwanted movements

The mean angles and standard deviations (*SD*) of the measurements in two conditions are given in tables 3 and 4. Appendix C shows the (+) and (-) angles alongside the mean and *SD*. Around the flexion-extension and radial-ulnar deviation axes, the *SD* was relatively small ( $SD < 4.3$  degrees). Outliers were found during both movements. During the flexion-extension, slight pronation and supination movements were observed.

Table 3: Flexion-extension - Mean angles and *SD*

		Flexion - Extension				
		Unloaded condition		Loaded condition		
(+)/(-)	Movement	Mean	SD	mean	SD	P
(+)	Extension	0.36	1.09	0.33	0.74	0.16
(-)	Flexion	-74.12	4.21	-64.07	6.66	<.001*
(+)	Ulnar deviation	2.53	2.62	2.87	1.81	0.31
(-)	Radial deviation	-2.60	0.60	-0.77	1.64	<.001*
(+)	Pronation	3.52	1.29	0.76	0.82	<.001*
(-)	Supination	-4.52	4.44	-2.74	3.70	0.13

+ = maximum; - = minimum; Movement = movements corresponding to the axes; Mean angles and *SD* for measurements with and without an anatomical specimen; P value of the Mann Whitney U test; \* = significant difference

Table 4: Radial-Ulnar Deviation - Mean angles and SD

Radial-Ulnar Deviation						
		Unloaded condition		Loaded condition		
(+)/(-)	Movement	Mean	SD	mean	SD	P
(+)	Extension	0.88	0.19	1.12	0.58	0.27
(-)	Flexion	-5.58	0.77	-2.67	1.30	<.001*
(+)	Ulnar deviation	22.58	2.27	3.75	2.77	<.001*
(-)	Radial deviation	-19.84	2.50	-1.83	3.00	<.001*
(+)	Pronation	3.21	0.42	0.32	0.60	<.001*
(-)	Supination	-1.65	0.54	-0.64	1.09	<.001*

+ = maximum; - = minimum; Movement = movements corresponding to the axes; Mean angles and SD for measurements with and without an anatomical specimen; P value of the Mann Whitney U test; \* = significant difference

### 3.2.1 Difference between the two conditions

The difference between the two conditions was measured with the (+) and (-) angles, these differences between conditions are shown in figures 11 to 14.

Not all values for each measurement were normally distributed ( $p < .05$ ), with skewness and kurtosis values exceeding -2 and +2. To determine if there was a difference in (+) and (-) angles during flexion-extension and radial-ulnar deviation in the two conditions, a series of Mann-Whitney U tests were performed.

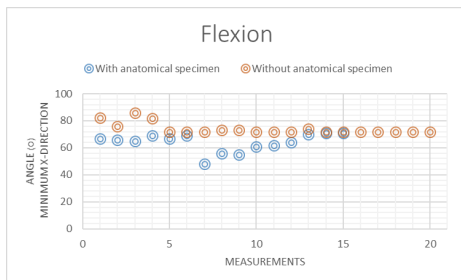


Figure 11: Flexion movement with and without an anatomical specimen

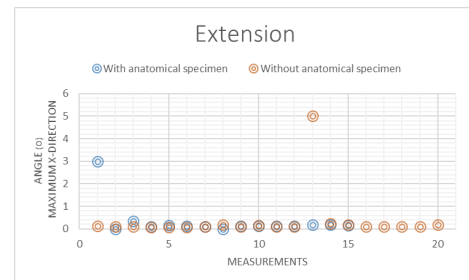


Figure 12: Extension movement with and without an anatomical specimen

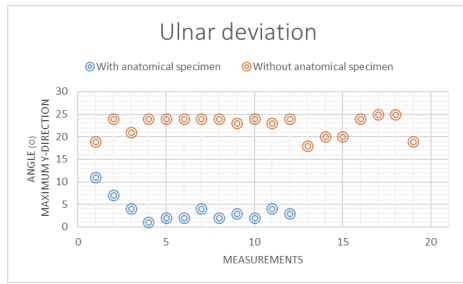


Figure 13: Ulnar deviation with and without an anatomical specimen

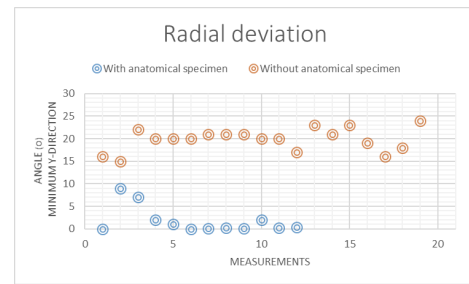
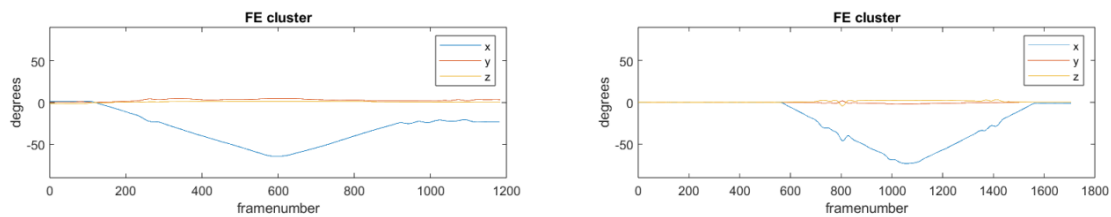


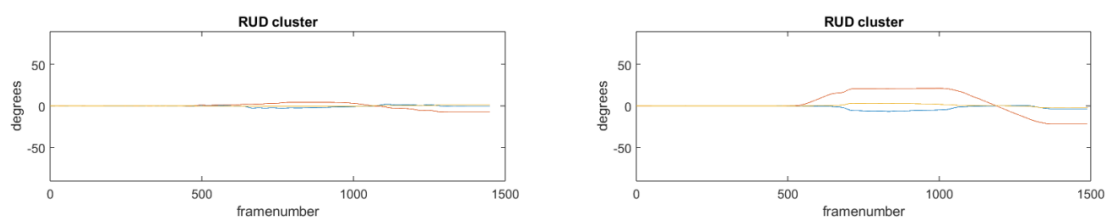
Figure 14: Radial deviation with and without an anatomical specimen

Data analysis in Matlab revealed discrepancies between the two conditions. The measurement in the unloaded condition returns to zero during extension, whereas the loaded condition falters and does not return to the starting point/zero, as shown in figure 15. For radial-ulnar deviation, the difference is even more obvious, seen in figure 16. Almost no movement is observed during the measurement in the loaded condition. This observation can also be seen in table 4, where the P-value of the Mann-Whitney U-test are shown. Significant differences ( $p < 0.05$ ) were found in almost all directions. Especially during radial-ulnar deviation.



left = Loaded condition; right = Unloaded condition

Figure 15: Difference between two conditions - flexion-extension



left = Loaded condition; right = Unloaded condition

Figure 16: Difference between two conditions - radial-ulnar deviation

### 3.2.2 Reliability of the movements generated by the motion guidance device

The reliability of the movements generated by the device was tested with an ICC. A low level of reliability was found between the two conditions during both flexion-extension and radial-ulnar deviation. The single measures ICC per movement with the 95% confi-

dence interval are displayed in table 5.

Table 5: ICC

Movement	Intraclass Correlation Coefficient values		
	Intraclass Correlation	95% Confidence Interval	
		Lower Bound	Upper Bound
Flexion	0.076	-0.100	0.375
Extension	-0.45	-0.583	0.480
Ulnar Deviation	-0.017	-0.022	0.035
Radial Deviation	-0.11	-0.027	0.061

After the ICC, Bland-Altman plots were generated to visualize the mean difference between the flexion-extension and radial-ulnar deviation angles between the two conditions. The blue line is the mean, and the dashed red lines are the lower and upper 95% limits.

These Bland-Altman plots visualize the agreement between the two conditions. In all directions, two or more samples fall outside the 95% limits, which means the (+) and (-) angles around all axes between conditions were not in agreement. The Bland-Altman plots for flexion-extension are shown in figures 17 to 18 and for radial-ulnar deviation in figures 19 and 20. The difference from zero was measured with a one-sample t-test. During both movements, the difference was significant, except for the extension, displayed in figure 17.

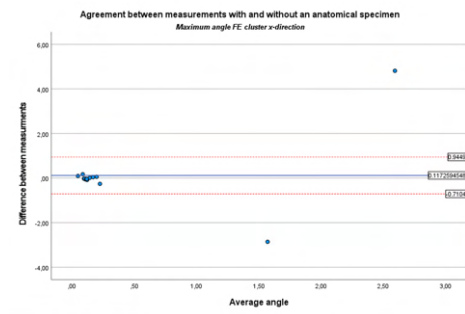


Figure 17: Agreement between measurements during flexion-extension

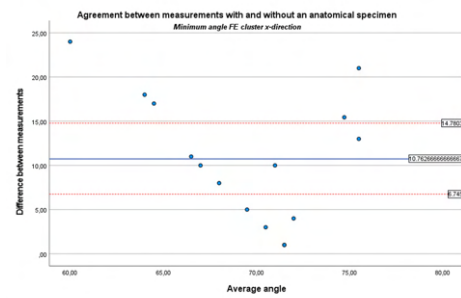


Figure 18: Agreement between measurements during flexion-extension

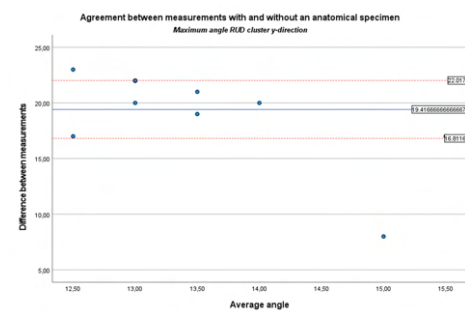


Figure 19: Agreement between measurements during radial-ulnar deviation

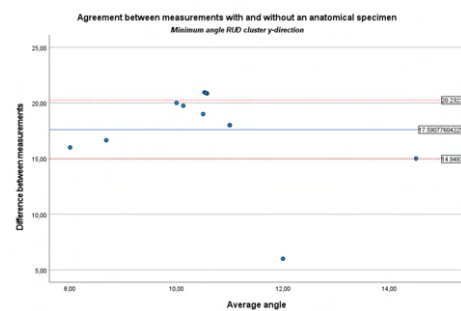


Figure 20: Agreement between measurements during radial-ulnar deviation

## 4 Discussion

The main aim of this research was to test the reliability of the movements and data generated by the device. It is hypothesized that the device would provide accurate results in the unloaded condition, but that a loaded condition may create resistance that the device can not handle. The results of the study shed light on the poor reliability of the movements generated by the motion guidance device in both conditions. To understand the results of this study, the research process is first reflected on, and the results are interpreted. Finally, suggestions are made for future research.

Three different tests were conducted: measurement of unwanted movements, the difference between a loaded and unloaded condition and the reliability of the movements generated by the device and how it was affected in the loaded condition. The findings are step by step explained and reflected on in the following paragraphs.

When measuring the movements to look for unwanted movements around all axes, there was considerably less movement during extension than was anticipated (mean =  $0.36^\circ$ ,  $SD = 1.09$ ), and there was little variation in between the maximum and minimum angles in the repeated measurements in the unloaded condition during flexion-extension.

Another interesting discovery is that the high  $SD$  during radial-ulnar deviation is caused by increased radial deviation, which causes less movement during ulnar deviation and vice versa (ulnar-deviation mean =  $22.58^\circ$   $SD = 2.27$  & radial-deviation mean =  $-19.84^\circ$ ,  $SD = 2.50$ ).

Unwanted movements around other axes than the flexion-extension axis were observed during flexion-extension around all axes, with a mean angle between  $-4.52^\circ$  and  $3.52^\circ$  in the unloaded condition,  $-2.74^\circ$  and  $2.87^\circ$  in the loaded condition. During radial-ulnar deviation, unwanted flexion was observed (mean =  $-5.58$   $SD = 0.77$ ) in the unloaded condition. Less unwanted movements were observed in the loaded condition. An explanation for this is the added weight in the loaded condition, which makes it harder for the device to rotate, which resulted in less movement of the device around all axes. These differing values can also be explained by a weak motor and loose timing belts, which causes vibrations during both flexion-extension and radial-ulnar deviation.

When comparing the movements generated by the device in the two conditions, significant differences were found around eight of the twelve axes. These significant differences suggest inconsistencies between the two conditions. During flexion-extension, significant differences were found around the flexion, radial deviation and pronation axes ( $P = <.001$ ). Significant differences were found during radial-ulnar deviation around all axes, ( $P = <.001$ ) except for the extension axes. One explanation for the differences found between the conditions is the weight added by the specimen. This caused faltering during extension, resulting in less movement. Virtually no movement was found in radial-ulnar deviation in the loaded condition.

In contrast to the hypothesis, significant differences were discovered in directions other than the anticipated flexion, extension, ulnar- and radial deviation axes. Not all the differences were significant in the anticipated directions of movement. There was no significant difference during the extension movement ( $P = 0.16$ ). This might be a result of the faltering and constrained extension movement seen during the experiment.

The Bland-Altman plots show that the differences between the measurements were well above zero, indicating that the movements generated by the device were not reliable. Furthermore, when interpreting the ICC data, a low degree of reliability was found between the unloaded and loaded condition for both flexion-extension and radial-ulnar deviation, which is in line with the other results.

Since this particular study has not been done before, it was challenging to connect it to the body of literature. In earlier experiments, patients were instructed to move their wrists or researchers used an unreliable motion guidance device to visualize wrist kinematics using a 4D CT scan (Rauch et al., 2018; White et al., 2019; Brinkhorst et al., 2022). In the literature, the reliability of these devices has not been examined. This study is a follow-up to the review by Crezee (2022), which found that the device can produce reliable wrist images during a 4D CT scan, but did not address the device's and images' test-retest reliability.

Throughout this research, several structural and mechanical issues were discovered. The motion guidance device was not made accessible until later in the course of the research. When it was available, it was discovered that the device did not function as the documentation suggested, necessitating adjustments. The planned testing date had to be postponed because it required additional time to develop and implement the adjustments. These adjustments are explained in section 2.1. Due to the availability of the required personnel, maintenance on the CT scanner, and necessary adjustments to the device, the test date was rescheduled four weeks after the initial date. Due to the four-week delay, there was not enough time for data analysis, which prevented CT images from being examined.

The limited period of time the anatomical specimens were available during the testing process was a source of concern. Time restrictions prevented the completion of the CT measuring protocol, which is included in the appendix B. Due to time constraints, only two of the five available specimens were scanned. Three radial-ulnar deviation measurements were disregarded because the Motive software's marker data was corrupt and might have produced inaccurate results, which could have contributed to incorrect conclusions.

It was discovered during testing that the anatomical specimen's weight had an impact on the flexion-extension and radial-ulnar deviation. Flexion-extension suffered from faltering and was unable to reach the movement's beginning position because of limited extension. Three of the five specimens showed no movement during radial-ulnar deviation, whereas the other specimen only moved little.

All in all, the research contributes to improve our knowledge of the motion guidance device's reliability during flexion-extension and radial-ulnar deviation. Adjustments to the

device are required to increase the device's reliability, according to the findings.

The main objective of future research should be to improve the device. The improvements should be focused on:

1. Adding stronger motors and tighter timing belts that are capable of supporting the weight of an anatomical specimen.
2. Consideration should be given to using stronger materials that can also be used in the CT scanner, since the pulleys and screws flex when subjected to the force and speed of the motors.
3. The radial-ulnar deviation mechanism needs to be optimized if the stronger motors are unable to resolve the issues.

Furthermore, it should also be examined whether the device's unreliability affects the test-retest reliability of the wrist kinematics by using the 4D CT-images to calculate the movements around the axes shown in table 1.

## 5 Conclusion

The aim of the research was to investigate the motion guidance device's reliability. The primary question was as follows: *Do the flexion-extension and radial-ulnar deviation, which are motor driven movements generated by the motion guidance device, provide reliable data in two conditions; unloaded and loaded?* The results show that there were unwanted movements observed in both conditions, less in the loaded condition. In addition, differences between the two conditions were found around almost all axes, which suggests that the added weight of an anatomical specimen is too much for the device to function. Furthermore, a low reliability was found between the two conditions.

This research showed that there were differences between repeated measurements during flexion-extension and radial-ulnar deviation with the motion guidance device in both conditions. The reliability of the device in both conditions was also measured, and it was concluded that the device did not provide reliable data. Without adjustments to improve the reliability of the motion guidance device, its use in future research on wrist kinematics is not recommended.

## References

- Andersson, J. K., Andernord, D., Karlsson, J., & Fridén, J. (2015, October). Efficacy of magnetic resonance imaging and clinical tests in diagnostics of wrist ligament injuries: A systematic review. *Arthroscopy*, *31*(10), 2014–20.e2.
- Brinkhorst, M., Foumani, M., van Rosmalen, J., Selles, R., Hovius, S., Strackee, S., & Streekstra, G. (2021, February). Quantifying in vivo scaphoid, lunate, and capitate kinematics using four-dimensional computed tomography. *Skeletal Radiol.*, *50*(2), 351–359.
- Brinkhorst, M., Foumani, M., van Rosmalen, J., Selles, R., Hovius, S., Strackee, S., & Streekstra, G. (2022, June). Four-dimensional CT analysis of carpal kinematics: An explorative study on the effect of sex and hand-dominance. *J. Biomech.*, *139*(110870), 110870.
- Crezee, W. (2022). *Development of a motion guidance device for 4D CT scans of the wrist*.
- de Roo, M. G. A., Dobbe, J. G. G., Peymani, A., van der Made, A. D., Strackee, S. D., & Streekstra, G. J. (2020, May). Accuracy of manual and automatic placement of an anatomical coordinate system for the full or partial radius in 3D space. *Sci. Rep.*, *10*(1), 8114.
- Giraudeau, B. (1996, October). Negative values of the intraclass correlation coefficient are not theoretically possible. *J. Clin. Epidemiol.*, *49*(10), 1205–1206.
- Jensen, J., Tromborg, H. B., Rasmussen, B. S. B., Gerke, O., Torfing, T., Precht, H., & Graumann, O. (2021, April). The effect of forearm rotation on radiographic measurements of the wrist: an experimental study using radiostereometric analyses on cadavers. *Eur. Radiol. Exp.*, *5*(1), 15.
- Kamal, R. N., Starr, A., & Akelman, E. (2016, October). Carpal kinematics and kinetics. *J. Hand Surg. Am.*, *41*(10), 1011–1018.
- Kawamura, K., & Chung, K. C. (2007, October). Management of wrist injuries. *Plast. Reconstr. Surg.*, *120*(5), 73e–89e.
- Koo, T. K., & Li, M. Y. (2016, June). A guideline of selecting and reporting intraclass correlation coefficients for reliability research. *J. Chiropr. Med.*, *15*(2), 155–163.
- Kwong, Y., Mel, A. O., Wheeler, G., & Troupis, J. M. (2015, October). Four-dimensional computed tomography (4DCT): A review of the current status and applications. *J. Med. Imaging Radiat. Oncol.*, *59*(5), 545–554.
- Mat Jais, I. S., Liu, X., An, K.-N., & Tay, S. C. (2014, December). A method for carpal motion hysteresis quantification in 4-dimensional imaging of the wrist. *Med. Eng. Phys.*, *36*(12), 1699–1703.
- Moojen, T. M., Snel, J. G., Ritt, M. J. P. F., Venema, H. W., Kauer, J. M. G., & Bos, K. E. (2003, January). In vivo analysis of carpal kinematics and comparative review of the literature. *J. Hand Surg. Am.*, *28*(1), 81–87.
- Myles, P. S., & Cui, J. (2007, September). Using the Bland-Altman method to measure agreement with repeated measures. *Br. J. Anaesth.*, *99*(3), 309–311.
- Prosser, R., Harvey, L., Lastayo, P., Hargreaves, I., Scougall, P., & Herbert, R. D. (2011).

Provocative wrist tests and MRI are of limited diagnostic value for suspected wrist ligament injuries: a cross-sectional study. *J. Physiother.*, 57(4), 247–253.

Rauch, A., Arab, W. A., Dap, F., Dautel, G., Blum, A., & Gondim Teixeira, P. A. (2018, December). Four-dimensional CT analysis of wrist kinematics during radioulnar deviation. *Radiology*, 289(3), 750–758.

White, J., Couzens, G., & Jeffery, C. (2019, November). The use of 4D-CT in assessing wrist kinematics and pathology: a narrative view. *Bone Joint J.*, 101-B(11), 1325–1330.

# Appendices

## A Measurement protocol *OptiTrack* measurement

## Experimental protocol – validity testing motion guidance device

Protocol Version	1.0
Study date	
Study Location	Reinier de Graaf Gasthuis
Goals of the study	To test the validity and test- retest reliability of a 4D CT scanning device for the wrist.
Participants	3 (5) cadaver arms

### Supplies

Wetlab EMC			
Check	Materials	Location	Responsible
<input type="checkbox"/>	3 (5) cadaveric specimens of the wrist	Wetlab EMC	Gerald
<input type="checkbox"/>	Covering material	Wetlab EMC	Gerald
RDGG Room			
Check	Materials	Location	Responsible
<input type="checkbox"/>	OptiTrack Flex (4 camera's)	HHS	Gwen
<input type="checkbox"/>	Reflective markers	HHS	Gwen
<input type="checkbox"/>	Tripod for each camera	HHS	Gwen
<input type="checkbox"/>	Table	RdGG	
<input type="checkbox"/>	External Hard Drive	TU/HHS	Gwen
<input type="checkbox"/>	Movement guidance Device		Gwen
<input type="checkbox"/>	Goniometer	RdGG (?)	
<input type="checkbox"/>	Tools to place specimen in device and attach (Velcro straps + Chinese fingers)		Gwen
<input type="checkbox"/>	Power Extension cord	RdGG	
<input type="checkbox"/>	Screwdriver and replacement parts for device + extra wires		Gwen
<input type="checkbox"/>	Tie wraps		
<input type="checkbox"/>	Duct-tape		
<input type="checkbox"/>	Laptop and charger		Gwen
<input type="checkbox"/>	USB-B to USB-A cable		Gwen
<input type="checkbox"/>	Photo-camera		Gwen
<input type="checkbox"/>	Notebook		Gwen
<input type="checkbox"/>	Gloves	RDGG	
<input type="checkbox"/>	Instant glue		Gwen
<input type="checkbox"/>	Plastic bags (for storage of anything)		Gwen
<input type="checkbox"/>	Permanent marker		Gwen

<input type="checkbox"/>	Table/trolley (for temporary storage of specimens)	RDGG	
<input type="checkbox"/>	Scissors		Gwen
<input type="checkbox"/>	Prints of this protocol		Gwen
<input type="checkbox"/>	Tools for cleaning	RDGG	
<input type="checkbox"/>			
<input type="checkbox"/>			

## Experimental protocol

*Place: CT room at RdGG*

*Participants: Three cadaver arms*

### 1. Set-up:

1. Set-up OptiTrack Flex
  - a. 4 OptiTrack camera's and 4 tripods
  - b. Place the other two camera's in an angle, looking on the device (figure 1)
  - c. Connect all the camera's with the HUB (appendix B.5)
  - d. Connect the HUB to the laptop and the power source
  - e. Calibrate the OptiTrack by wandng and setting a ground plane
2. Set-up motion guidance device
  - a. Follow the manual included in appendix B.6
  - b. Test the device by performing the FE and RUD movements

### 2. Positional accuracy measurements:

1. Attach power to the device (by plugging it into the extension cord)
2. Move device to location 1 (see table I)
3. Measure the location reached with a goniometer and note in table I (appendix B.1)
4. Reset location and repeat measurement twice
5. Repeat step 2.2-2.4 for all 4 locations

### 3. Marker placement:

1. Place the markers on the device (appendix B.4)
  - a. Secure the marker with tape
2. Test the marker visibility

### 4. Validity measurement without cadaver arm:

1. Measurement without specimen – FE movement (Appendix B.2)
2. Repeat 4.1
3. Measurement without specimen – RUD movement (Appendix B.2)
4. Repeat 4.3

### 5. Specimen:

1. Wear gloves
2. Place specimen 1 in the device with the hand palm surrounding the white bar
3. Attach specimen to device with Velcro straps and Chinese fingers

### 6. Validity measurement with cadaver arm:

1. Measurement with anatomical specimen – FE movement (Appendix B.2)

2. Repeat 6.1
3. Measurement with anatomical specimen – RUD movement (Appendix B.2)
4. Repeat 6.3
- 7. Replace specimen:**
  1. Remove power
  2. Detach specimen 1 from device
  3. Place specimen 2 in device as described in step 5. (Place Specimen)
  4. Place the markers on the specimen as described in appendix B.4
  5. Test the marker visibility
  6. (Repeat 8.2 – 5 for specimen 3(,4 and 5))
- 8. Repeat steps 7 for specimen 2 to 5**
- 9. End experiment:**
  1. OptiTrack
    - a. Assure the device is disconnected before unplugging
    - b. Export the C3D data to a laptop
  2. Motion guidance device
    - a. Remove power
    - b. Detach last specimen
    - c. Clean up device
    - d. Cover and store specimens

*B.1 Table 1 – accuracy measurement*

Location	Angle
1 (flexion)	
1 (flexion)	
2 (extension)	
2 (extension)	
3 (ulnar deviation)	
3 (ulnar deviation)	
4 (radial deviation)	
4 (radial deviation)	

*B.2 - Measurements – Table 2*

Measurement	Movement	With/without hand	Plane
1	FE	With specimen	Sagittal
2	FE	With specimen	Sagittal
3	FE	With specimen	Sagittal
4	RUD	With specimen	Frontal
5	RUD	With specimen	Frontal
6	RUD	With specimen	Frontal

*B.3 - Checklist measurements – Table 3*

Measurement	Measurement completed ?	Notes
-------------	-------------------------	-------

1	<input type="checkbox"/>	
2	<input type="checkbox"/>	
3	<input type="checkbox"/>	
4	<input type="checkbox"/>	
5	<input type="checkbox"/>	
6	<input type="checkbox"/>	
1	<input type="checkbox"/>	
2	<input type="checkbox"/>	
3	<input type="checkbox"/>	
4	<input type="checkbox"/>	
5	<input type="checkbox"/>	
6	<input type="checkbox"/>	
1	<input type="checkbox"/>	
2	<input type="checkbox"/>	
3	<input type="checkbox"/>	
4	<input type="checkbox"/>	
5	<input type="checkbox"/>	
6	<input type="checkbox"/>	
1	<input type="checkbox"/>	
2	<input type="checkbox"/>	
3	<input type="checkbox"/>	
4	<input type="checkbox"/>	
5	<input type="checkbox"/>	
6	<input type="checkbox"/>	
1	<input type="checkbox"/>	
2	<input type="checkbox"/>	
3	<input type="checkbox"/>	
4	<input type="checkbox"/>	
5	<input type="checkbox"/>	
6	<input type="checkbox"/>	

#### *B.4 – Marker placement*

<b>Markers *3 makers per set</b>	<b>Location</b>
Cluster set 1	Rotation axis RUD (on device)
Cluster set 2	Rotation axis FE (on device)
Cluster set 3	Device

## B.5 – Position OptiTrack



## B.6 – Manual motion guidance device

# Manual motion guidance device

Step 1: check if all the components are in the box (figure 1).

- the device
- breadboard
- power supply
- USB-A to USB-B

Step 2: check if the belt systems are connected properly

Step 3: connect the wires to the breadboard (figure 2 and 3)

Step 4: connect the wires from the device to the power supply (figure 2 and 4)

Step 5: tighten the screws on the power supply

Step 5: check if all the wires are connected

- the green LED lights up when everything is connected correctly (fig 4.A)

Step 6: test the range of motion of the device

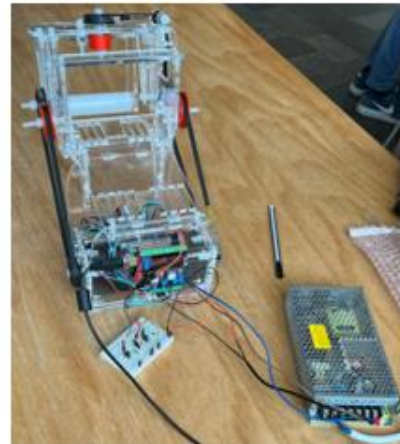


Figure 1: Motion guidance device

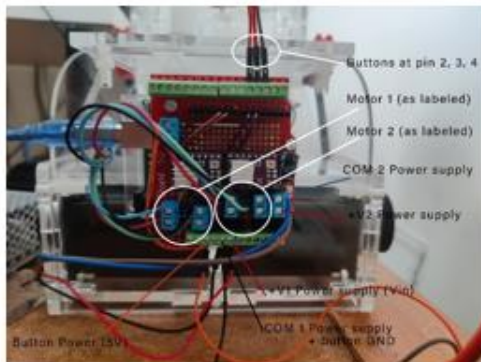


Figure 2: wiring device

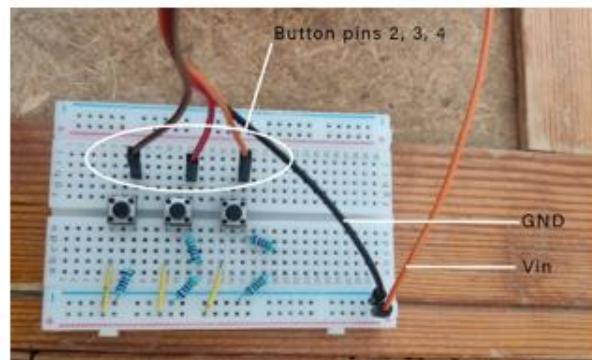


Figure 3: wiring device

Step 6: plug the USB-A in the Arduino and USB-B in the laptop

Step 7 (only if the script has never been downloaded before):

Download library:



Figure 4: Power supply

<https://www.arduino.cc/reference/en/libraries/accelstepper/>

Step 8: upload the Arduino script, check whether there are error messages

Step 9: plug the device in the power outlet

Step 10: test the movements (FE and RUD)

Step 11: run the device

## **B Measurement protocol 4D CT**

## Cadaver Study Protocol Evaluation 4D CT scan device

Protocol Version	4.0
Study date	
Study Location	Reinier de Graaf Gasthuis
Goals of the study	To test the validity and reliability of a 4D CT scanning device for the wrist.
Participants	

## Supplies

Wetlab EMC			
Check	Materials	Location	Responsible
<input type="checkbox"/>	5 cadaveric specimens of the wrist	Wetlab EMC	
<input type="checkbox"/>	Covering material	Wetlab EMC	
RDGG CT Room			
Check	Materials	Location	Responsible
<input type="checkbox"/>	CT Scanner	RDGG	
<input type="checkbox"/>	External Hard Drive	TU	
<input type="checkbox"/>	Motion guidance Device		
<input type="checkbox"/>	Tools to place specimen in device and attach (Velcro straps + Chinese fingers)		
<input type="checkbox"/>	Power Extension cord		
<input type="checkbox"/>	Screwdriver and replacement parts for device + extra wires		
<input type="checkbox"/>	1x Board to place device on		
<input type="checkbox"/>	Tie wraps		
<input type="checkbox"/>	Duct-tape		
<input type="checkbox"/>	Laptop and charger		
<input type="checkbox"/>	USB-B to USB-A cable		
<input type="checkbox"/>	Photo-camera		
<input type="checkbox"/>	Notebook		
<input type="checkbox"/>	Gloves	RDGG	
<input type="checkbox"/>	Instant glue		
<input type="checkbox"/>	Plastic bags (for storage of anything)		
<input type="checkbox"/>	Permanent marker		
<input type="checkbox"/>	Table/trolley (for temporary storage of specimens)	RDGG	
<input type="checkbox"/>	Scissors		
<input type="checkbox"/>	Prints of this protocol		
<input type="checkbox"/>	Tools for cleaning	RDGG	
<input type="checkbox"/>			
<input type="checkbox"/>			

**Room:** CT room at the RDGG

**Participants:** three anatomical specimen

1. Setup:
  1. Cover the CT table
  2. Place Board
  3. Make sure all wires of the device are attached correctly (Appendix C.4)
  4. Place Device on board and attach with tie wraps in the holes drilled in the board and at the bottom of the feet of the device. (Appendix C.5)
2. Place Specimen
  1. Wear gloves
  2. Place specimen 1 in the device with the hand palm surrounding the white bar
  3. Attach specimen to device with Velcro straps and Chinese fingers
3. Positional accuracy measurements
  1. Attach power to the device (by plugging it into the extension cord)
  2. Move device to location 1 (see table I)
  3. Measure the location reached with a goniometer and note in table I
  4. Reset location and repeat measurement twice
  5. Repeat step 3.2-3.4 for all 4 locations
4. 4D CT scans
  1. Place device with specimen on the board in the CT scanner
  2. Make a 4D CT scan of non-moving wrist with low radiation dosage (See appendix C.3 for scan protocol)
  3. Check table II
  4. Make a 4D CT scan of non-moving wrist with default radiation dosage (See appendix C.3 for scan protocol)
  5. Check table II
  6. Let the device perform Flexion/Extension (FE) with low speed ( $27^\circ$  per second)
  7. Make 4D CT scan of moving wrist with low speed (See appendix C.3 for scan protocol)
  8. Check table II
  9. Let the device perform Ulnar/Radial Deviation (URD) with low speed ( $27^\circ$  per second)
  10. Make 4D CT scan of moving wrist with low speed (See appendix C.3 for scan protocol)
  11. Check table II
5. Repeat step 4 (two scans per specimen completed? skip this step and go to 6 (Replace specimen)):
6. Replace specimen:
  1. Remove power
  2. Detach specimen 1 from device
  3. Place specimen 2 in device as described in step 2. (Place Specimen)
  4. Repeat step 3. (Positional accuracy measurements) for and step 4 (4D CT scans) for specimen 2
  5. Repeat step 5.1-5.4 for specimen 3(,4 and 5)

7. End of experiment
  1. Remove power
  2. Detach last specimen
  3. Clean up device, CT table and CT room
  4. Copy CT files to external hard drive
  5. Cover and store specimens

C.1 Table 1 – accuracy measurement

<b>Location</b>	<b>Angle</b>
1 (flexion)	
1 (flexion)	
2 (extension)	
2 (extension)	
3 (ulnar deviation)	
3 (ulnar deviation)	
4 (radial deviation)	
4 (radial deviation)	

C.2 Table 2

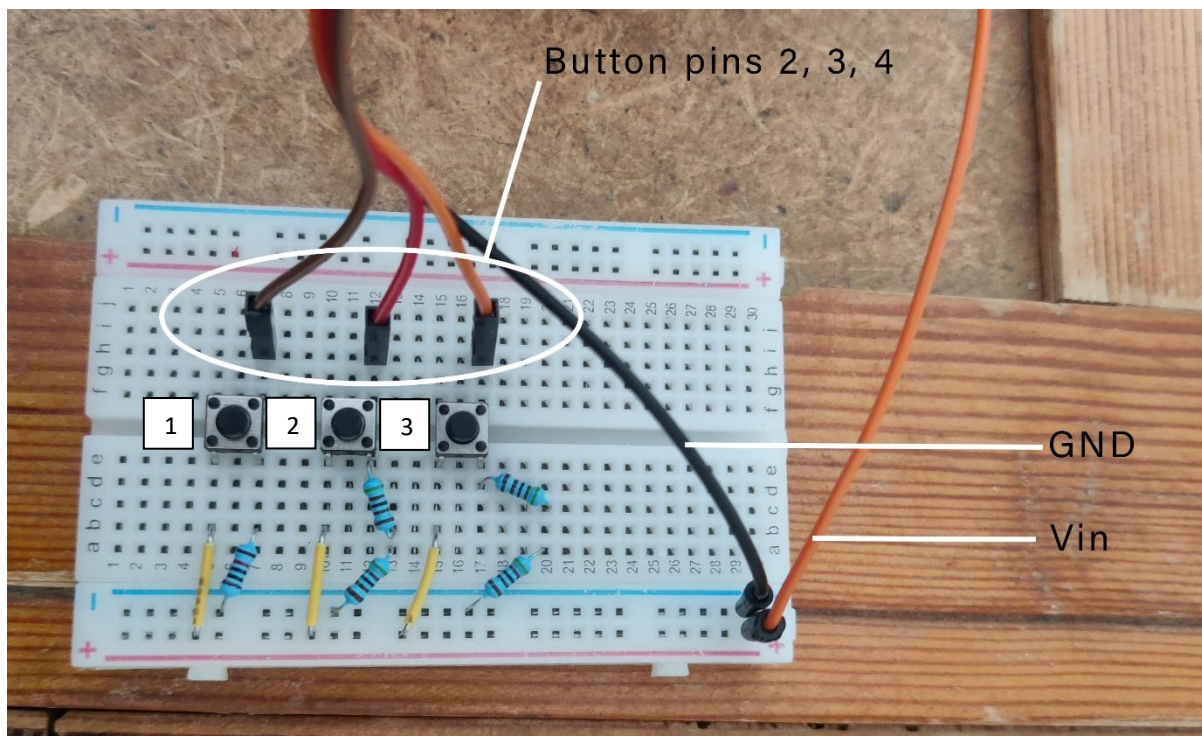
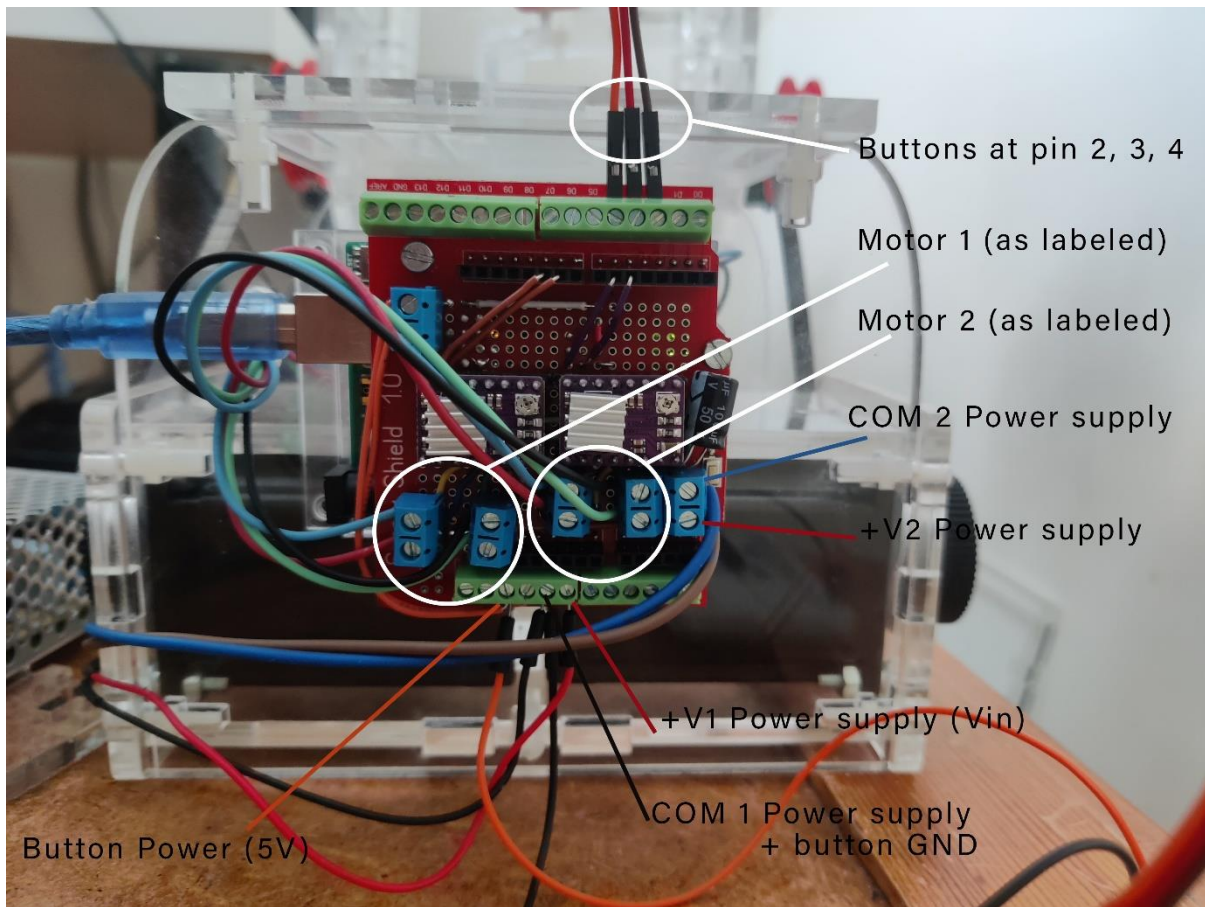
Ct Scan	Done?	Notes
Specimen 1 FE	<input type="checkbox"/>	
Specimen 1 FE	<input type="checkbox"/>	
Specimen 1 RUD	<input type="checkbox"/>	
Specimen 1 RUD	<input type="checkbox"/>	
Specimen 2 FE	<input type="checkbox"/>	
Specimen 2 FE	<input type="checkbox"/>	
Specimen 2 RUD	<input type="checkbox"/>	
Specimen 2 RUD	<input type="checkbox"/>	
Specimen 3 FE	<input type="checkbox"/>	
Specimen 3 FE	<input type="checkbox"/>	
Specimen 3 RUD	<input type="checkbox"/>	
Specimen 3 RUD	<input type="checkbox"/>	
Specimen 4 FE	<input type="checkbox"/>	
Specimen 4 FE	<input type="checkbox"/>	
Specimen 4 RUD	<input type="checkbox"/>	
Specimen 4 RUD	<input type="checkbox"/>	
Specimen 5 FE	<input type="checkbox"/>	
Specimen 5 FE	<input type="checkbox"/>	
Specimen 5 RUD	<input type="checkbox"/>	
Specimen 5 RUD	<input type="checkbox"/>	

### Appendix C.3: CT default dosage

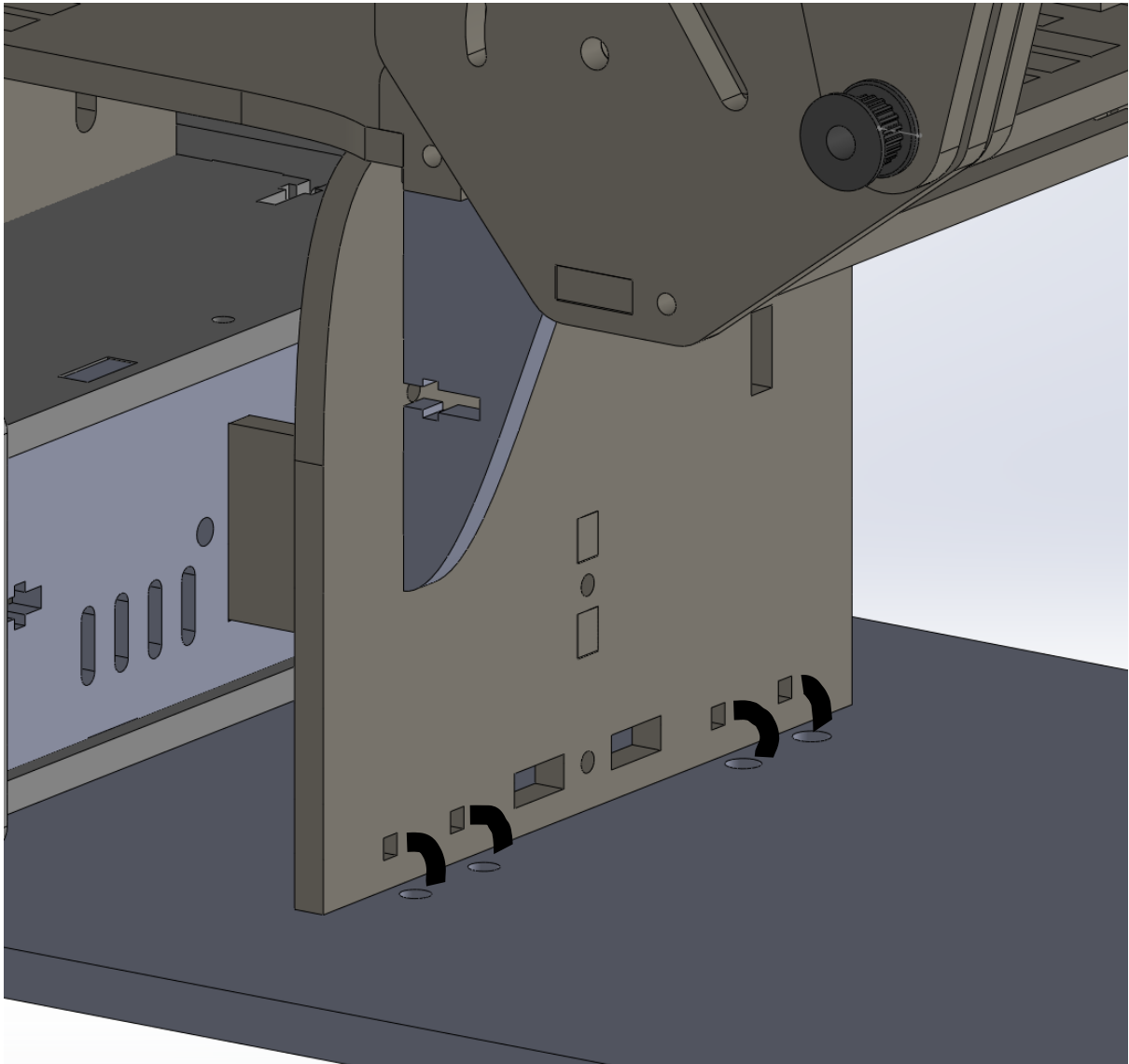
default radiation dosage

<b>Variable</b>	<b>Value</b>
Tube Current	15 mA
Tube Potential	80 kV
Total ScanTime	12.6 s
Range	140.0 mm
DFoV	120.0 mm

## Appendix C.4: Arduino Wiring



Appendix C.5: Board placement with tie wraps



## C All results

Table 6: FE - means and SD - without specimen

	Direction (X,Y,Z)	Minimum	Maximum	Mean	Std. Deviation
MAXFE	x	0,08	5,00	0,3607	1,09278
MINFE	x	86,00	72,00	74,1222	4,21146
MAXFE	y	0,00	11,00	2,5256	2,62169
MINFE	y	-4,00	-2,00	-2,6000	0,59824
MAXFE	z	1,00	7,00	3,5232	1,29106
MINFE	z	-18,00	-0,01	-4,5244	4,44068
MAXRUD	x	0,07	0,31	0,1260	0,06251
MINRUD	x	-75,00	-71,00	-71,9000	1,02084
MAXRUD	y	1,00	5,00	2,5073	1,51234
MINRUD	y	-6,00	-1,65	-3,9324	0,98522
MAXRUD	z	3,00	5,00	3,8500	0,67082
MINRUD	z	-4,00	0,00	-0,9613	0,87195
MAXDevice	x	0,00	0,05	0,0179	0,01695
MINDevice	x	-0,04	0,00	-0,0211	0,01247
MAXDevice	y	0,02	0,34	0,1613	0,08592
MINDevice	y	-0,21	-0,01	-0,1144	0,06144
MAXDevice	z	0,00	0,06	0,0143	0,01345
MINDevice	z	-0,05	0,00	-0,0147	0,01414
N (listwise)	20				

Table 7: FE - means and SD - with specimen

	Direction (X,Y,Z)	Minimum	Maximum	Mean	Std. Deviation
MAXFE	x	0,00	3,00	0,3281	0,74349
MINFE	x	-71,00	-48,00	-64,0667	6,65976
MAXFE	y	1,00	8,00	2,8667	1,80739
MINFE	y	-6,00	0,00	-0,7686	1,63918
MAXFE	z	0,00	3,00	0,7579	0,81979
MINFE	z	-15,00	0,00	-2,7427	3,70070
MAXRUD	x	0,01	6,00	0,6885	1,50740
MINRUD	x	-69,00	-43,00	-60,4000	7,78093
MAXRUD	y	0,00	5,00	2,7339	1,66656
MINRUD	y	-9,00	0,00	-2,3056	2,83308
MAXRUD	z	0,00	11,00	2,1811	3,01205
MINRUD	z	-6,00	-0,32	-1,9888	1,94884
N (listwise)	15				

Table 8: RUD - means and SD - without specimen

	Direction (X,Y,Z)	Minimum	Maximum	Mean	Std. Deviation
MAXFE	x	0,21	4,00	2,1605	1,47624
MINFE	x	-2,00	-0,80	-1,1648	0,44788
MAXFE	y	0,03	1,00	0,5640	0,36147
MINFE	y	-0,80	-0,11	-0,2583	0,17497
MAXFE	z	0,04	0,94	0,1773	0,20002
MINFE	z	-0,90	-0,06	-0,1914	0,18092
MAXRUD	x	0,24	1,00	0,8821	0,19448
MINRUD	x	-7,00	-5,00	-5,5789	0,76853
MAXRUD	y	18,00	25,00	22,5789	2,26852
MINRUD	y	-24,00	-15,00	-19,8421	2,50029
MAXRUD	z	3,00	4,00	3,2105	0,41885
MINRUD	z	-2,00	-0,46	-1,6527	0,53714
MAXDevice	x	0,00	0,04	0,0135	0,00914
MINDevice	x	-0,03	0,00	-0,0089	0,00699
MAXDevice	y	0,04	0,20	0,1156	0,04419
MINDevice	y	-0,04	0,00	-0,0056	0,01007
MAXDevice	z	0,00	0,03	0,0124	0,00952
MINDevice	z	-0,04	0,00	-0,0183	0,01193
N (listwise)	20				

Table 9: RUD - means and SD - with specimen

	Direction (X,Y,Z)	Minimum	Maximum	Mean	Std. Deviation
MAXFE	x	0,00	1,00	0,6339	0,36799
MINFE	x	-3,00	-1,00	-2,0833	0,66856
MAXFE	y	0,00	1,00	0,3451	0,40397
MINFE	y	-0,49	0,00	-0,2999	0,13544
MAXFE	z	0,00	0,70	0,1072	0,19511
MINFE	z	-0,92	-0,04	-0,2567	0,31107
MAXRUD	x	0,21	2,00	1,1169	0,57844
MINRUD	x	-5,00	-1,00	-2,6667	1,30268
MAXRUD	y	1,00	11,00	3,7500	2,76751
MINRUD	y	-9,00	0,00	-1,8259	3,00334
MAXRUD	z	0,00	2,00	0,3195	0,59742
MINRUD	z	-4,00	-0,06	-0,6403	1,08526
N (listwise)	12				

## D Matlab script

```

1 clearvars
2 close all
3 format short g
4 addpath(genpath(pwd)) % deze code zorgt ervoor dat alle submappen
5 % van je huidige folder(Current Folder) aan het matlab path worden toegevoegd

```

```

6 % inlezen c3d file
7 [fileName , pathName] = uigetfile('.c3d');
8 c3dfile = fullfile(pathName,fileName);
9 itf = c3dserver();
10 C3DStruct = get3dtargetsBT(itf,c3dfile);
11
12 %% Lowpass filteren
13 cutoff = 5;
14 order = 4;
15 framerate = 120;
16 ClusterNames = string(fieldnames(C3DStruct));
17 % eerst de namen van de clusters vinden om die te kunnen gebruiken in de
18 % loop
19 % lowpass filter toepassen op alle markerdata (for-loop)
20 for i = 2:length(ClusterNames) % beginnen vanaf 2, sloth 1 is altijd 'info'
21     C3DStruct.(ClusterNames(i)).Marker1 = LowPassData(C3DStruct.(ClusterNames(i)
22     ).Marker1,framerate,order,cutoff);
23     C3DStruct.(ClusterNames(i)).Marker2 = LowPassData(C3DStruct.(ClusterNames(i)
24     ).Marker2,framerate,order,cutoff);
25     C3DStruct.(ClusterNames(i)).Marker3 = LowPassData(C3DStruct.(ClusterNames(i)
26     ).Marker3,framerate,order,cutoff);
27 end
28
29 %% transformatie matrices maken voor elk cluster in een for-loop
30 NumFrames = length(C3DStruct.RUD.Marker1);
31 for i = 2:length(ClusterNames)
32     for j = 1:NumFrames
33         C3DStruct.(ClusterNames(i)).TransMat(:, :, j) = CalcTransMat(C3DStruct.(
34         ClusterNames(i)).Marker1(j, :),C3DStruct.(ClusterNames(i)).Marker2(j, :),
35         C3DStruct.(ClusterNames(i)).Marker3(j, :));
36     end
37 end
38
39 %% clusters visualiseren (nog niet uitgelijnd)
40 % plot_clusters(C3DStruct.(ClusterNames(2)).TransMat,C3DStruct.(ClusterNames(3))
41     .TransMat,C3DStruct.(ClusterNames(4)).TransMat)
42 % waitfor(findobj('-regex','Tag','clusterplot')) % wait until previous gui
43     closes
44
45 %% Transformatiematrix voor de referentiehouding maken
46 RefFrame=120;%(een seconde na de start van de meting)
47 for i = 2:length(ClusterNames) % begin bij 2 want field 1 heet altijd info
48     C3DStruct.(ClusterNames(i)).Ref(:, :, 1) =C3DStruct.(ClusterNames(i)).TransMat
49     (:, :, RefFrame);
50 end
51
52 %% Clusters uitlijnen met het globale assenstelsel.
53 for i = 2:length(ClusterNames) % begin bij 2 want field 1 heet altijd info
54     for j = 1:NumFrames % voor elk frame dus hier wel bij 1 beginnen
55         C3DStruct.(ClusterNames(i)).TransMat_RelRef(:, :, j) =zeros(4,4);
56     end
57 end
58
59 %% het rotatiedeel (3x3) gebruiken voor de vermenigvuldiging met de inverse van

```

```

frame 120
49 % A*inv(B) = A/B
50 % daarna in dezelfde loop de positie van de origin van de transmat matrices in
    kolom 4 van de nieuwe matrices zetten.
51 for i = 2:length(ClusterNames) % begin bij 2 want field 1 heet altijd info
52     for j = 1:NumFrames % deze teller start wel bij 1 want je wilt alle frames
        van de meting hebben natuurlijk
53         C3DStruct.(ClusterNames(i)).TransMat_RelRef(1:3,1:3,j) = C3DStruct.(
            ClusterNames(i)).TransMat(1:3,1:3,j)/C3DStruct.(ClusterNames(i)).Ref
                (1:3,1:3);
54         C3DStruct.(ClusterNames(i)).TransMat_RelRef(:,4,j) = C3DStruct.(
            ClusterNames(i)).TransMat(:,4,j);
55     end
56 end
57 %% clusters visualiseren(nu netjes uitgelijnd in frame 120)
58 % plot_clusters(C3DStruct.(ClusterNames(2)).TransMat_RelRef,C3DStruct.(
        ClusterNames(3)).TransMat_RelRef,C3DStruct.(ClusterNames(4)).TransMat_RelRef
        )
59 % waitfor(findobj('-regex','Tag','clusterplot')) % wait until previous gui
        closes
60
61 %% matrices maken die de orientatie van de segmenten tov elkaar weergeven
62 for i = 1: NumFrames
63     C3DStruct.RUDa(:, :, i) = C3DStruct.(ClusterNames(2)).TransMat_RelRef(:, :, i)\
        C3DStruct.(ClusterNames(4)).TransMat_RelRef(:, :, i);
64     C3DStruct.FEa(:, :, i) = C3DStruct.(ClusterNames(3)).TransMat_RelRef(:, :, i)\
        C3DStruct.(ClusterNames(4)).TransMat_RelRef(:, :, i);
65     C3DStruct.Devicea(:, :, i) = C3DStruct.(ClusterNames(4)).TransMat_RelRef(:, :, i
        );
66 end
67
68 % plot_clusters(C3DStruct.Devicea)
69 % waitfor(findobj('-regex','Tag','clusterplot')) % wait until previous gui
        closes
70
71 %% Euler hoeken uit de matrices herleiden met decompositie volgorde x,z,y
72 RUDAngleR1 = zeros(NumFrames,3);
73 RUDAngleR2 = zeros(NumFrames,3);
74 FEAngleR1 = zeros(NumFrames,3);
75 FEAngleR2 = zeros(NumFrames,3);
76 DeviceAngleR1 = zeros(NumFrames,3);
77 DeviceAngleR2 = zeros(NumFrames,3);
78
79 for i = 1: NumFrames
80     [RUDAngleR1(i,:),RUDAngleR2(i,)] = RotationMatrixToCardanicAngles(C3DStruct.
        RUDa(:, :, i), [1 2 3]); % X Z Y
81     [FEAngleR1(i,:),FEAngleR2(i,)] = RotationMatrixToCardanicAngles(C3DStruct.
        FEa(:, :, i), [1 2 3]); % X Z Y
82     [DeviceAngleR1(i,:),DeviceAngleR2(i,)] = RotationMatrixToCardanicAngles(
        C3DStruct.Devicea(:, :, i), [1 2 3]); % X Z Y
83 end

```

```

84 %% Plot xyz data in degrees
85 DeviceAngleR3 = (DeviceAngleR1*180/pi);
86 RUDAngleR3 = (RUDAngleR1*180/pi);
87 FEAngleR3 = (FEAngleR1*180/pi);
88
89 figure(1)
90 subplot(3,1,1)
91 plot(RUDAngleR3)
92 ylabel('degrees')
93 xlabel('framenumber')
94 title('RUD movement')
95 subplot(3,1,2)
96 plot(FEAngleR3)
97 ylabel('degrees')
98 xlabel('framenumber')
99 title('FE movement')
100 subplot(3,1,3)
101 plot(DeviceAngleR3)
102 ylabel('degrees')
103 xlabel('framenumber')
104 title('Device movement')
105
106 %% xyz angle data set in a new variable
107 %FE movement
108 DataXDirectionFE = (FEAngleR3(:,1));
109 DataYDirectionFE = (FEAngleR3(:,2));
110 DataZDirectionFE = (FEAngleR3(:,3));
111 %RUD movement
112 DataXDirectionRUD = (RUDAngleR3(:,1));
113 DataYDirectionRUD = (RUDAngleR3(:,2));
114 DataZDirectionRUD = (RUDAngleR3(:,3));
115 %Device movement
116 DataXDirectionDevice = (DeviceAngleR3(:,1));
117 DataYDirectionDevice = (DeviceAngleR3(:,2));
118 DataZDirectionDevice = (DeviceAngleR3(:,3));
119
120 %Aanvullen met markerdata hand/pols
121
122 %% maxima and minima data FE, RUD & Device + plot
123 %% FE cluster movement
124 % x-direction
125 [pksFEpx,indxFEpx] = findpeaks(DataXDirectionFE,'MinPeakHeight',10,'
    MinPeakDistance',100); % x direction
126 [pksFEdx,indxFEdx] = findpeaks(-DataXDirectionFE,'MinPeakHeight',50,'
    MinPeakDistance',10);
127 smallPeakIndexesFEpx = pksFEpx < 5; %Removing all peaks below a certain point
128 pksFEpx(smallPeakIndexesFEpx) = [] ; %Reject Y value of peaks below this
    threshold
129 indxFEpx(smallPeakIndexesFEpx) = [] ; %Reject Y value of peaks below this
    threshold
130

```

```

131 smallPeakIndexesFEdx = pksFEdx < 5; %Removing all peaks below a certain point
132 pksFEdx(smallPeakIndexesFEdx) = [] ; %Reject Y value of peaks below this
    threshold
133 indxFEdx(smallPeakIndexesFEdx) = [] ; %Reject Y value of peaks below this
    threshold
134 figure (5)
135 sgtitle('FE cluster movement')
136 subplot(3,1,1)
137
138 plot(DataXDirectionFE)
139 title('FE - x-direction')
140 ylabel('degrees')
141 xlabel('framenumbers')
142 ylim([-90,90])
143 hold on
144
145 plot(indxFEpx, pksFEpx, 'o')
146 plot(indxFEdx, -pksFEdx, 'o')
147
148 %y-direction
149 [pksFEpy,indxFEpy] = findpeaks(DataYDirectionFE,'MinPeakHeight',0,'
    MinPeakDistance',100); %y-direction
150 [pksFEpy,indxFEpy] = findpeaks(-DataYDirectionFE,'MinPeakDistance',100);
151 smallPeakIndexesFEpy = pksFEpy < 5; %Removing all peaks below a certain point
152 pksFEpy(smallPeakIndexesFEpy) = [] ; %Reject Y value of peaks below this
    threshold
153 indxFEpy(smallPeakIndexesFEpy) = [] ; %Reject Y value of peaks below this
    threshold
154
155 smallPeakIndexesFEpy = pksFEpy < 5; %Removing all peaks below a certain point
156 pksFEpy(smallPeakIndexesFEpy) = [] ; %Reject Y value of peaks below this
    threshold
157 indxFEpy(smallPeakIndexesFEpy) = [] ; %Reject Y value of peaks below this
    threshold
158 subplot(3,1,2)
159
160 plot(DataYDirectionFE)
161 title('RUD - y-direction')
162 ylabel('degrees')
163 xlabel('framenumbers')
164 ylim([-90,90])
165 hold on
166
167 plot(indxFEpy, pksFEpy, 'o')
168 plot(indxFEpy, -pksFEpy, 'o')
169
170 %z-direction
171 [pksFEpz,indxFEpz] = findpeaks(DataZDirectionFE,'MinPeakHeight',1,'
    MinPeakDistance',100); %y-direction
172 [pksFEpz,indxFEpz] = findpeaks(-DataZDirectionFE,'MinPeakDistance',100);
173

```

```

174 smallPeakIndexesFEpz = pksFEpz < 5; %Removing all peaks below a certain point
175 pksFEpz (smallPeakIndexesFEpz) = [] ; %Reject Y value of peaks below this
    threshold
176 indxFEpz (smallPeakIndexesFEpz) = [] ; %Reject Y value of peaks below this
    threshold
177
178 smallPeakIndexesFEdz = pksFEdz < 5; %Removing all peaks below a certain point
179 pksFEdz (smallPeakIndexesFEdz) = [] ; %Reject Y value of peaks below this
    threshold
180 indxFEdz (smallPeakIndexesFEdz) = [] ; %Reject Y value of peaks below this
    threshold
181 subplot (3,1,3)
182
183 plot (DataZDirectionFE)
184 title ('Device - z-direction')
185 ylabel ('degrees')
186 xlabel ('framenumber')
187 ylim ([-90,90])
188 hold on
189
190 plot (indxFEpz, pksFEpz, 'o')
191 plot (indxFEdz, -pksFEdz, 'o')
192
193 hold off
194 %% RUD cluster movement
195 [pksRUDpx,indxRUDpx] = findpeaks (DataXDirectionRUD,'MinPeakHeight',5,'
    MinPeakDistance',100); % x direction
196 [pksRUDDx,indxRUDDx] = findpeaks (-DataXDirectionRUD,'MinPeakHeight',5,'
    MinPeakDistance',10);
197
198 smallPeakIndexesRUDpx = pksRUDpx < 5; %Removing all peaks below a certain point
199 pksRUDpx (smallPeakIndexesRUDpx) = [] ; %Reject Y value of peaks below this
    threshold
200 indxRUDpx (smallPeakIndexesRUDpx) = [] ; %Reject Y value of peaks below this
    threshold
201
202 smallPeakIndexesRUDDx = pksRUDDx < 5; %Removing all peaks below a certain point
203 pksRUDDx (smallPeakIndexesRUDDx) = [] ; %Reject Y value of peaks below this
    threshold
204 indxRUDDx (smallPeakIndexesRUDDx) = [] ; %Reject Y value of peaks below this
    threshold
205
206 figure (6)
207 sgtitle ('RUD cluster movement')
208 subplot (3,1,1)
209
210 plot (DataXDirectionRUD)
211 title ('FE - x-direction')
212 ylabel ('degrees')
213 xlabel ('framenumber')
214 ylim ([-200,90])

```

```

215 hold on
216
217 plot(indxRUDpx, pksRUDpx, 'o')
218 plot(indxRUDdx, -pksRUDdx, 'o')
219
220 %y-direction
221 [pksRUDpy,indxRUDpy] = findpeaks(DataYDirectionRUD,'MinPeakHeight',0,'
    MinPeakDistance',100); %y-direction
222 [pksRUddy,indxRUddy] = findpeaks(-DataYDirectionRUD,'MinPeakDistance',100);
223
224 smallPeakIndexesRUDpy = pksRUDpy < 5; %Removing all peaks below a certain point
225 pksRUDpy(smallPeakIndexesRUDpy) = [] ; %Reject Y value of peaks below this
    threshold
226 indxRUDpy(smallPeakIndexesRUDpy) = [] ; %Reject Y value of peaks below this
    threshold
227
228 smallPeakIndexesRUddy = pksRUddy < 5; %Removing all peaks below a certain point
229 pksRUddy(smallPeakIndexesRUddy) = [] ; %Reject Y value of peaks below this
    threshold
230 indxRUddy(smallPeakIndexesRUddy) = [] ; %Reject Y value of peaks below this
    threshold
231 subplot(3,1,2)
232
233 plot(DataYDirectionRUD)
234 title('RUD - y-direction')
235 ylabel('degrees')
236 xlabel('framenumber')
237 ylim([-200,90])
238 hold on
239
240 plot(indxRUDpy, pksRUDpy, 'o')
241 plot(indxRUddy, -pksRUddy, 'o')
242
243 %z-direction
244 [pksRUDpz,indxRUDpz] = findpeaks(DataZDirectionRUD,'MinPeakHeight',0,'
    MinPeakDistance',100); %y-direction
245 [pksRUddz,indxRUddz] = findpeaks(-DataZDirectionRUD,'MinPeakDistance',100);
246
247 smallPeakIndexesRUDpz = pksRUDpz < 5; %Removing all peaks below a certain point
248 pksRUDpz(smallPeakIndexesRUDpz) = [] ; %Reject Y value of peaks below this
    threshold
249 indxRUDpz(smallPeakIndexesRUDpz) = [] ; %Reject Y value of peaks below this
    threshold
250
251 smallPeakIndexesRUddz = pksRUddz < 5; %Removing all peaks below a certain point
252 pksRUddz(smallPeakIndexesRUddz) = [] ; %Reject Y value of peaks below this
    threshold
253 indxRUddz(smallPeakIndexesRUddz) = [] ; %Reject Y value of peaks below this
    threshold
254 subplot(3,1,3)
255

```

```

256 plot(DataZDirectionRUD)
257 title('Device - z-direction')
258 ylabel('degrees')
259 xlabel('framenumber')
260 ylim([-200,90])
261 hold on
262
263 plot(indxRUDpz, pksRUDpz, 'o')
264 plot(indxRUDdz, -pksRUDdz, 'o')
265
266 hold off
267 %% Device cluster movement
268 [pksDevicepx,indxDevicepx] = findpeaks(DataXDirectionDevice,'MinPeakDistance'
    ,100); % x direction
269 [pksDevedcx,indxDevedcx] = findpeaks(-DataXDirectionDevice,'MinPeakDistance'
    ,10);
270
271 smallPeakIndexesDevicepx = pksDevicepx < 5; %Removing all peaks below a certain
    point
272 pksDevicepx(smallPeakIndexesDevicepx) = [] ; %Reject Y value of peaks below this
    threshold
273 indxDevicepx(smallPeakIndexesDevicepx) = [] ; %Reject Y value of peaks below
    this threshold
274
275 smallPeakIndexesDevedcx = pksDevedcx < 5; %Removing all peaks below a certain
    point
276 pksDevedcx(smallPeakIndexesDevedcx) = [] ; %Reject Y value of peaks below this
    threshold
277 indxDevedcx(smallPeakIndexesDevedcx) = [] ; %Reject Y value of peaks below
    this threshold
278
279 figure (7)
280 sgtitle('Device cluster movement')
281 subplot(3,1,1)
282
283 plot(DataXDirectionDevice)
284 title('FE - x-direction')
285 ylabel('degrees')
286 xlabel('framenumber')
287 ylim([-90,90])
288 hold on
289
290 plot(indxDevicepx, pksDevicepx, 'o')
291 plot(indxDevedcx, -pksDevedcx, 'o')
292
293 %y-direction
294 [pksDevicepy,indxDevicepy] = findpeaks(DataYDirectionDevice,'MinPeakHeight',0,'
    MinPeakDistance',100); %y-direction
295 [pksDevedcy,indxDevedcy] = findpeaks(-DataYDirectionDevice,'MinPeakDistance'
    ,100);
296

```

```

297 smallPeakIndexesDevicecy = pksDevicecy < 5; %Removing all peaks below a certain
    point
298 pksDevicecy (smallPeakIndexesDevicecy) = [] ; %Reject Y value of peaks below this
    threshold
299 indxDevicecy (smallPeakIndexesDevicecy) = [] ; %Reject Y value of peaks below
    this threshold
300
301 smallPeakIndexesDevedcy = pksDevedcy < 5; %Removing all peaks below a certain
    point
302 pksDevedcy (smallPeakIndexesDevedcy) = [] ; %Reject Y value of peaks below this
    threshold
303 indxDevedcy (smallPeakIndexesDevedcy) = [] ; %Reject Y value of peaks below
    this threshold
304
305 subplot (3,1,2)
306
307 plot (DataYDirectionDevice)
308 title ('RUD - y-direction')
309 ylabel ('degrees')
310 xlabel ('framenumber')
311 ylim ([-90,90])
312 hold on
313
314 plot (indxDevicecy, pksDevicecy, 'o')
315 plot (indxDevedcy, -pksDevedcy, 'o')
316
317 %z-direction
318 [pksDevicecz,indxDevicecz] = findpeaks (DataZDirectionDevice,'MinPeakDistance'
    ,100);
319 [pksDevedcz,indxDevedcz] = findpeaks (-DataZDirectionDevice,'MinPeakDistance'
    ,100);
320
321 smallPeakIndexesDevicecz = pksDevicecz < 5; %Removing all peaks below a certain
    point
322 pksDevicecz (smallPeakIndexesDevicecz) = [] ; %Reject Y value of peaks below this
    threshold
323 indxDevicecz (smallPeakIndexesDevicecz) = [] ; %Reject Y value of peaks below
    this threshold
324
325 smallPeakIndexesDevedcz = pksDevedcz < 5; %Removing all peaks below a certain
    point
326 pksDevedcz (smallPeakIndexesDevedcz) = [] ; %Reject Y value of peaks below this
    threshold
327 indxDevedcz (smallPeakIndexesDevedcz) = [] ; %Reject Y value of peaks below
    this threshold
328
329 subplot (3,1,3)
330
331 plot (DataZDirectionDevice)
332 title ('Device - z-direction')
333 ylabel ('degrees')

```

```

334 xlabel('framenumber')
335 ylim([-90,90])
336 hold on
337
338 plot(indxDevicepz, pksDevicepz, 'o')
339 plot(indxDevicedz, -pksDevicedz, 'o')
340
341 hold off
342
343 %% ROM xyz direction for FE, RUD and device movement
344
345 ROMXFE = max(DataXDirectionFE) - min(DataXDirectionFE);
346 ROMYFE = max(DataYDirectionFE) - min(DataYDirectionFE);
347 ROMZFE = max(DataZDirectionFE) - min(DataZDirectionFE);
348
349 ROMXRUD = max(DataXDirectionRUD) - min(DataXDirectionRUD);
350 ROMYRUD = max(DataYDirectionRUD) - min(DataYDirectionRUD);
351 ROMZRUD = max(DataZDirectionRUD) - min(DataZDirectionRUD);
352
353 ROMXDevice = max(DataXDirectionDevice) - min(DataXDirectionDevice);
354 ROMYDevice = max(DataYDirectionDevice) - min(DataYDirectionDevice);
355 ROMZDevice = max(DataZDirectionDevice) - min(DataZDirectionDevice);
356
357 %Aanvullen met markerdata hand/pols

```

## E Arduino script

```

1 #include <AccelStepper.h>
2 #include <MultiStepper.h>
3
4 //Button Pins
5 #include <AccelStepper.h> //download the Accellstepper from the internet if the
   script doesn't work.
6
7
8 #define dirPin_1 10
9 #define stepPin_1 9
10
11 #define dirPin_2 6
12 #define stepPin_2 5
13
14 const int stepsPerRev = 200; //Number of steps per output rotation
15 #define motorInterfaceType 1
16
17 // Create a new instance of the AccelStepper class:
18 AccelStepper stepper_1 = AccelStepper(motorInterfaceType, stepPin_1, dirPin_1);
19 AccelStepper stepper_2 = AccelStepper(motorInterfaceType, stepPin_2, dirPin_2);
20
21 #define btn1 2
22 #define btn2 3

```

```

23 #define btn3 4
24 const int buttonInterval = 70; // debouncing for too short press
25
26 int lastSteadyState_1 = LOW; // the previous steady state from the input
    pin 1
27 int lastSteadyState_2 = LOW; // the previous steady state from the input
    pin 2
28 int lastSteadyState_3 = LOW; // the previous steady state from the input
    pin 3
29 int lastFlickerableState_1 = LOW; // the previous flickerable state from the
    input pin 1
30 int lastFlickerableState_2 = LOW; // the previous flickerable state from the
    input pin 2
31 int lastFlickerableState_3 = LOW; // the previous flickerable state from the
    input pin 3
32 int currentState_1; // the current reading from the input pin 1
33 int currentState_2; // the current reading from the input pin 2
34 int currentState_3; // the current reading from the input pin 3
35 int t_delay = 400;
36 int w_delay = 8000;
37 int speed = 10;
38 unsigned long previousButtonMillis = 0;
39 int Button_state = 0; // last state of the button: 0, 1, 2 or 3
40
41 unsigned long t_debounce_1 = 0; //last time output pin 1 was toggled
42 unsigned long t_debounce_2 = 0;
43 unsigned long t_debounce_3 = 0;
44
45
46 void setup() {
47     pinMode(btn1, INPUT);
48     pinMode(btn2, INPUT);
49     pinMode(btn3, INPUT);
50
51     stepper_1.setMaxSpeed(50);
52     stepper_2.setMaxSpeed(500);
53     stepper_1.setSpeed(15); //movement speed device (motor steps per second)
54     stepper_2.setSpeed(15); //movement speed device (motor steps per second)
55
56     Serial.begin(9600);
57 }
58
59 void loop() {
60
61     Serial.print("buttonstate = ");
62     Serial.println(Button_state);
63     rest();
64     rest_2();
65     FlexionExtension();
66     UlnairRadialDeviation();
67     readButtons();

```

```

68 }
69
70 void rest_2() { //after each movement this state is implemented, except for the
    default position
71 if (Button_state == 0) {
72
73     Serial.println("resting");
74 }
75 }
76
77 void rest() { // push this button if you want the device to go back to the
    default position from RUD movement
78 if (Button_state == 1) {
79     Serial.println("Default position");
80     delay(t_delay);
81     //stepper_1.setCurrentPosition(0);
82     //if (stepper_1.currentPosition() != 0)
83     //{
84         //stepper_1.setSpeed(speed);
85         //stepper_1.runSpeed();
86     //}
87
88     //stepper_2.setCurrentPosition(0);
89     if (stepper_2.currentPosition() != -20) //20
90     {
91         stepper_2.setSpeed(speed);
92         stepper_2.runSpeed();
93     }
94     //Button_state = 0;
95 }
96 }
97
98 void FlexionExtension() {
99     if (Button_state == 2) {
100         Serial.println("pause");
101         delay(8000);
102         Serial.println("Performing FE");
103         stepper_1.setCurrentPosition(0);
104         while (stepper_1.currentPosition() != -40)
105         {
106             stepper_1.setSpeed(-speed);
107             stepper_1.runSpeed();
108         }
109
110         delay(t_delay); //change to w_delay when performing the accuracy measurement
111
112         stepper_1.setCurrentPosition(0);
113
114         // Run the motor backwards at 600 steps/second until the motor reaches -200
115         // steps (1 revolution):
116         while (stepper_1.currentPosition() != 40)

```

```

116     {
117         stepper_1.setSpeed(speed);
118         stepper_1.runSpeed();
119     }
120     Button_state = 0;
121     delay(t_delay);
122 }
123 }
124
125 void UlnairRadialDeviation() {
126     if (Button_state == 3) {
127
128         Serial.println("Pause");
129         delay(8000);
130         Serial.println("Performing URD");
131
132         stepper_2.setCurrentPosition(0);
133         while (stepper_2.currentPosition() != 40)
134         {
135             stepper_2.setSpeed(speed);
136             stepper_2.runSpeed();
137         }
138
139         delay(t_delay); // change to w_delay when performing the accuracy
140                         // measurement
141
142         // Reset the position to 0:
143         stepper_2.setCurrentPosition(0);
144
145         // Run the motor backwards at 600 steps/second until the motor reaches -200
146         // steps (1 revolution):
147         while (stepper_2.currentPosition() != -40)
148         {
149             stepper_2.setSpeed(-speed);
150             stepper_2.runSpeed();
151         }
152         Button_state = 0;
153         delay(t_delay);
154     }
155 }
156
157 void readButtons() {
158     if (millis() - previousButtonMillis >= buttonInterval) {
159
160         if (digitalRead(btn1) == HIGH) {
161             Button_state = 1;
162             Serial.println ("Button 1");
163             previousButtonMillis += buttonInterval;
164         }
165         else if (digitalRead(btn2) == HIGH) {
166             Button_state = 2;

```

```
165     Serial.println ("Button 2");
166     previousButtonMillis += buttonInterval;
167 }
168 else if (digitalRead(btn3) == HIGH) {
169     Button_state = 3;
170     Serial.println ("Button 3");
171     previousButtonMillis += buttonInterval;
172 }
173 }
174
175
176 }
```

## F Planning

Weken	Planning
1 (6 feb – 10 feb) 40 uur	Oriëntatie onderwerp + projectplan schrijven
2 (13 feb – 17 feb) 40 uur	Meelopen poli + OK Projectplan schrijven  DEADLINE projectplan (16 feb – 18:00)
3 (20 feb – 24 feb) 40 uur	Training 3D Slicer Literatuuronderzoek Feedback verwerken projectplan PPRO-assessment (23 feb 9:00 – 9:30)
Krokusvakantie (27 feb – 3 maart) 40 uur	Doorwerken Training 3D Slicer Literatuuronderzoek + specificeren methode
4 (6 maart – 10 maart) 40 uur	Meelopen poli + OK Feedback verwerken projectplan DEADLINE ext. herkansing projectplan (10 maart – 18:00)
5 (13 maart – 17 maart) 40 uur	Meelopen
6 (20 maart – 24 maart) 40 uur	Metingen? Afstemmen met Nina + Gerald
7 (27 maart – 31 apr) 40 uur	Metingen? Afstemmen met Nina + Gerald
8 (3 apr – 7 apr) 40 uur	Metingen? Afstemmen met Nina + Gerald
9 (10 apr – 14 apr)	Vakantie
10 (17 apr – 21 apr) 40 uur	Dataverwerking 3D Slicer Data beoordelen en doorsturen naar andere beoordelaars
11 (24 apr – 28 apr) 40 uur	Dataverwerking in SPSS
12 (1 mei – 5 mei) 40 uur	Dataverwerking in SPSS
13 (8 mei – 12 mei) 40 uur	Resultaten schrijven
14 (15 mei – 19 mei) 40 uur	Limitatie' s en discussie
15 (22 mei – 26 mei) 40 uur	Discussie en conclusie
16 (29 mei – 2 juni) 40 uur	DEADLINE '0' versie scriptie (31 mei – 12:00)
17 (5 juni – 9 juni) 40 uur	Verwerken feedback
18 (12 juni – 16 juni) 40 uur	Conceptversie scriptie (14 juni – 12:00)